Physics – Uspekhi **47** (12) 1205 – 1220 (2004)

REVIEWS OF TOPICAL PROBLEMS PACS numbers: 42.65.Dr, 42.65.Ky, 42.65.Re, 42.65.Wi

Isolated waveguide modes of high-intensity light fields

A M Zheltikov

DOI: 10.1070/PU2004v047n12ABEH001917

Contents

Abstract. Isolated waveguide modes of intense light fields are unique physical objects, which can never be observed in standard optical fibers, hollow waveguides, plasma filaments, or in the bulk of a transparent dielectric or gas. Hollow photonic-crystal fibers can for the first time produce robust isolated truly guided spatial modes of subgigawatt ultrashort light pulses, perform efficient nonlinear-optical transformations of laser fields in such states, and implement new waveguide regimes of coherent excitation and probing of molecular Raman-active modes in the gas phase.

1. Introduction

Nonlaser sources of light generate electromagnetic radiation by spontaneously emitting uncorrelated photons at random instants of time in arbitrary directions (Fig. 1a). Nondirected incoherent light has been the main subject of optics for more than two millennia, from the Hellenistic epoch of antiquity [1] until the laser era. Stimulated emission of light, predicted by Einstein in 1916 [2] and experimentally observed for the first time by Ladenburg in 1928 [3], suggests the way to generate directed electromagnetic waves (Fig. 1b). The search for practical sources of optical radiation based on stimulated emission had been on for more than two decades, culminating in the creation of masers and lasers in the 1950s [4 – 6] (Table 1).

Laser sources, where the emission of photons is stimulated by an external electromagnetic field, can generate highly coherent, well-directed radiation (Fig. 1b). Transmission of laser radiation over large distances is, however, inhibited by diffraction — an intrinsic property of light related to its wave nature, which has been systematically studied by many scholars since Fresnel [7]. As early as 1910, long before the invention of the laser, Hondros and Debye [8] theoretically examined the possibility of reducing the diffraction-induced divergence of light due to the total internal reflection — the phenomenon that gives rise to guided modes of electromagnetic radiation in dielectric waveguides (Fig. 1c). Progress in laser science and the advent of highly transparent materials in the 1970s (Table 1) have stimulated a rapid growth in fiber optics, allowing the creation of high-performance optical telecommunication lines and development of fiber-optic components for the control of laser radiation [9 – 11].

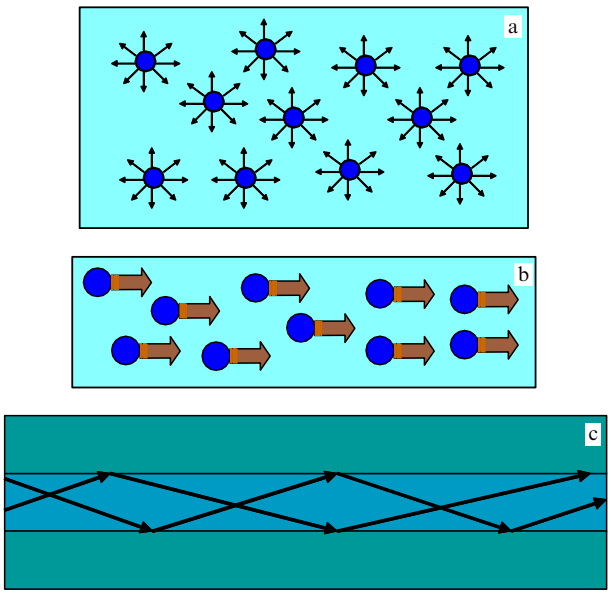

Figure 1. Nondirected incoherent radiation of a nonlaser source (a), directed coherent laser radiation (b), and guided-wave transmission of laser radiation (c).

A M Zheltikov Physics Department, International Laser Center, M V Lomonosov Moscow State University, Vorob'evy gory, 119992 Moscow, Russian Federation
Tel. (7-095) 939 51 74. Fax: (7-095) 939 31 13
E-mail: zheltikov@phys.msu.ru

Received 9 June 2004, revised 21 July 2004
Uspekhi Fizicheskikh Nauk **174** (12) 1301 – 1318 (2004)
Translated by A M Zheltikov; edited by M V Magnitskaya

Table 1. From optics and catoptrics of nondirected light to guided-wave high-intensity light fields: fundamental problems of transmission of high-intensity laser radiation in isolated guided modes and their solutions.

Problems	Solutions
Nondirected radiation emission (Euclid, 300 BC [1], through the entire pre-laser era)	Stimulated emission (Einstein, 1916 [2]); Lasers (Basov, Prokhorov, Townes, Maiman, 1950s [4 – 6])
Diffraction (Fresnel, 1815 [7])	Step-index guiding (Hondros, Debye, 1910 [8]; fiber-optic breakthrough of the 1970s [9 – 11])
Self-focusing leading to optical breakdown (early 1960s [13 – 20])	Hollow waveguides (Miles et al., 1977 [30]; Nisoli et al., 1996 [23])
Alternative of standard hollow waveguides: multimode guiding or unacceptably high losses	Hollow photonic-crystal fibers (Russell, 1999 [41, 42])

The rise of high-power laser systems capable of generating light pulses with intensities up to 10^{23} W cm^{-2} [12] has revealed fundamental physical limitations on the laser power that can be transmitted as guided modes in the bulk of a transparent dielectric. These limitations originate from self-focusing [13 – 20], related to an intensity-dependent radial profile of the refractive index

$$n(r) = n_0 + n_2 I(r)$$

(n_0 is the refractive index of the material in the absence of laser radiation and n_2 is the nonlinear refractive index), induced by the laser beam with an intensity distribution $I(r)$ nonuniform in the transverse coordinate r. Such a profile of the refractive index is equivalent to a nonlinear lens, leading to a collapse of the laser beam and an optical breakdown of the material.

The critical power of self-focusing for radiation with a wavelength λ propagating in a medium with a nonlinear refractive index n_2 is given by [20]

$$P_c = \frac{\lambda^2}{8\pi n_0 n_2} .$$

For a nonlinear refractive index $n_2 \approx 3 \times 10^{-16}$ cm^2 W^{-1}, typical of fused silica, we arrive at the following estimate on the critical power of self-focusing: $P_c \approx 1$ MW. Dielectric waveguides, thus, cannot guide laser pulses with powers exceeding P_c.

Hollow waveguides [21] are a powerful and convenient tool for the transmission and nonlinear-optical transformation of high-power laser pulses (Table 1). The threshold of optical breakdown for gases filling the core of such waveguides is much higher than typical breakdown thresholds for dielectrics, with the radiation fluence on the waveguide walls usually being several orders of magnitude lower than the radiation fluence at the center of the waveguide core. Due to this advantageous combination of properties, hollow waveguides have made it possible to perform several interesting and important experiments dealing with the physics of high-intensity ultrashort laser pulses [22]. Hollow-core fibers are intensely used, in particular, in modern laser systems to increase the length of nonlinear-optical interactions of laser pulses and to enhance nonlinear-optical processes. Fibers of this type allow ultrashort laser pulses to be spectrally transformed through nonlinear-optical processes without a laser breakdown in the fiber core.

Self-phase modulation (SPM) in a gas filling the core of a hollow fiber makes it possible to produce pulses shorter than 5 fs [23, 24]. Stimulated Raman scattering (SRS) of laser pulses in hollow fibers filled with Raman-active gases results in an efficient generation of multiple Raman sidebands. In the regime of locked phases, these Raman sidebands can be employed to synthesize pulses shorter than 4 fs [25]. Hollow waveguides can radically enhance high-order harmonic generation [26 – 29] and improve the sensitivity of gas-phase analysis based on four-wave mixing (FWM) spectroscopy [30 – 34].

The modes of standard hollow fibers with a solid dielectric cladding are leaky [21], with the magnitude of optical losses increasing for these modes as λ^2/a^3 with a decrease in the radius a of the hollow core (λ is the radiation wavelength). There is no way, therefore, to use standard hollow fibers with very small inner diameters for laser experiments, which usually operate with hollow fibers with core diameters ranging from 100 up to 500 μm. Such fibers are essentially multimode. The losses of guided modes in standard, solid-cladding hollow fibers with smaller core diameters are typically unacceptably high for the transmission and nonlinear-optical transformations of laser pulses.

We thus arrive at the following alternative for standard hollow waveguides with a solid dielectric cladding: the waveguides of this class are either unacceptably lossy or multimode for electromagnetic radiation in the optical range of wavelengths. The difference in phase and group velocities of waveguide modes simultaneously excited in a standard hollow fiber gives rise to uncertainties in time-resolved measurements and complicates the calibration of the nonlinear signal as a function of the gas pressure [32]. Thus, although conventional, solid-cladding hollow fibers can provide very high levels of nonlinear signals, quantitative analysis of gas-phase media and time-resolved measurements based on nonlinear-optical processes in such fibers often encounter serious difficulties.

Filamentation of high-intensity ultrashort laser pulses, induced by the spatial and temporal self-action of laser radiation and ionization of the gas medium [35 – 37], is another interesting waveguiding option, allowing the channeling of terawatt- and multiterawatt-level laser radiation over large distances. This phenomenon can provide high efficiencies of nonlinear-optical spectral transformation of high-power ultrashort laser pulses, giving rise to radiation emission within a very broad spectral range (supercontinuum) [38] and offering unique possibilities in remote sensing of the atmosphere, with a typical range of this technique reaching several kilometers [39, 40]. The laser beam dynamics in filaments is, however, very complicated. The light field generally undergoes uncontrollable amplitude- and phase-profile transformations and distortions in this regime, indicating an effective cross-talk between multiple spatial modes of the field and apparently leaving no way for a selective manipulation of individual guided modes, as many applications would require.

Isolated waveguide modes of intense light fields are, thus, unique physical objects, which cannot be observed in standard optical fibers, hollow waveguides, plasma filaments, or in the bulk of a transparent dielectric or gas. We will show in this review that the recently created hollow-core

photonic-crystal fibers (PCFs) [41–45] can for the first time produce robust isolated truly guided spatial modes of subgigawatt ultrashort light pulses (see Table 1) and can perform efficient nonlinear-optical transformations of such states of electromagnetic field.

Hollow PCFs confine guided modes of electromagnetic radiation within the low-index area of the hollow core due to the high reflectivity of a two-dimensionally periodic (photonic-crystal) cladding within photonic band gaps (PBGs) [41–46]. In these frequency ranges, an electromagnetic field cannot exist in the form of waves propagating inside the periodic structure of the photonic-crystal cladding. The reflection coefficient of a periodic structure within PBGs is much higher than the reflection coefficient of the material of the cladding, substantially reducing optical losses of air-guided modes in hollow fibers. Photonic band gaps of the PCF cladding are mapped onto passbands in fiber transmission.

Due to the high intensities of laser pulses achieved in the hollow core of PCFs without an optical breakdown of the fiber and because of the large interaction length provided by the waveguide geometry, hollow PCFs can radically enhance nonlinear-optical processes, including stimulated Raman scattering [47, 48], four-wave mixing [49], and self-phase modulation [50]. As demonstrated by experiments [51, 52], hollow PCFs can transmit ultrashort laser pulses in the regime of temporal solitons. Such fibers can be employed for the laser guiding of microspecies and atoms [53], as well as for the transportation of high-energy laser pulses for technological [54, 55] and biomedical [56] applications.

The plan of this review is as follows. In Section 2, we provide simple qualitative geometric-optic arguments to illustrate the physical mechanisms behind the formation of guided modes in hollow waveguides with a periodic cladding. Based on this analysis, we will demonstrate the possibility of a radical lowering of losses, typical of hollow waveguides, due to the high reflectivity of the periodic cladding of the waveguide. In Section 3, we examine the properties of guided modes in hollow PCFs by numerically solving the wave equation for the electromagnetic field in the fiber. Section 4 is devoted to frequency-nondegenerate nonlinear-optical interactions of ultrashort laser pulses in hollow PCFs. We will show in this section that hollow PCFs with a special dispersion profile can phase-match nonlinear-optical interactions of isolated air-guided modes of high-power femtosecond laser pulses.

In Section 5, we discuss the self-channeling of high-intensity ultrashort laser pulses in hollow PCFs. Section 6 outlines ways of a radically enhancing coherent anti-Stokes Raman scattering (CARS) in isolated air-guided modes of hollow PCFs. Section 7 explores the possibilities of using hollow PCFs for enhancing high-order harmonic generation. The main results are briefly summarized in the Conclusion.

2. Photonic band gaps, photonic crystals, and reduced optical losses of hollow waveguides

In conventional fibers, guided modes of electromagnetic radiation are produced through total internal reflection. In hollow waveguides, however, the refractive index of the core is lower than the refractive index of the cladding. The propagation constants of waveguide modes in such a situation have nonzero imaginary parts. Optical losses are, thus, inherent in air-guided modes of hollow waveguides. This circumstance limits the waveguide length in nonlinear-optical experiments, imposing restrictions on the enhancement of the nonlinear signal generated through harmonic generation or wave mixing.

In this section, we will show that the use of hollow waveguides with a periodic cladding allows optical losses inherent in hollow-waveguide modes to be considerably reduced. The field of electromagnetic radiation in periodic structures has the form of Bloch waves [57]. The existence of frequency ranges where the incident light wave becomes resonantly coupled with reflected waves, prohibiting the solution to the field equations in the form of Bloch waves propagating inside the structure, is the fundamental property of periodic media. An insightful and consistent description of this phenomenon can already be found in Bragg's dynamic diffraction theory [58]. For natural crystals, the condition of a strong coupling between the forward and reflected waves is known as the Bragg condition [58]:

$$2d \sin\theta = m\lambda\,.$$

For a given integer m, this condition relates the angle 2θ between the incident and reflected beams (Fig. 2a) to the distance d between crystallographic planes and the radiation wavelength λ.

By analogy with natural crystals, providing conditions of Bragg diffraction for X-rays, structures displaying a spatially periodic modulation of the refractive index on a spatial scale

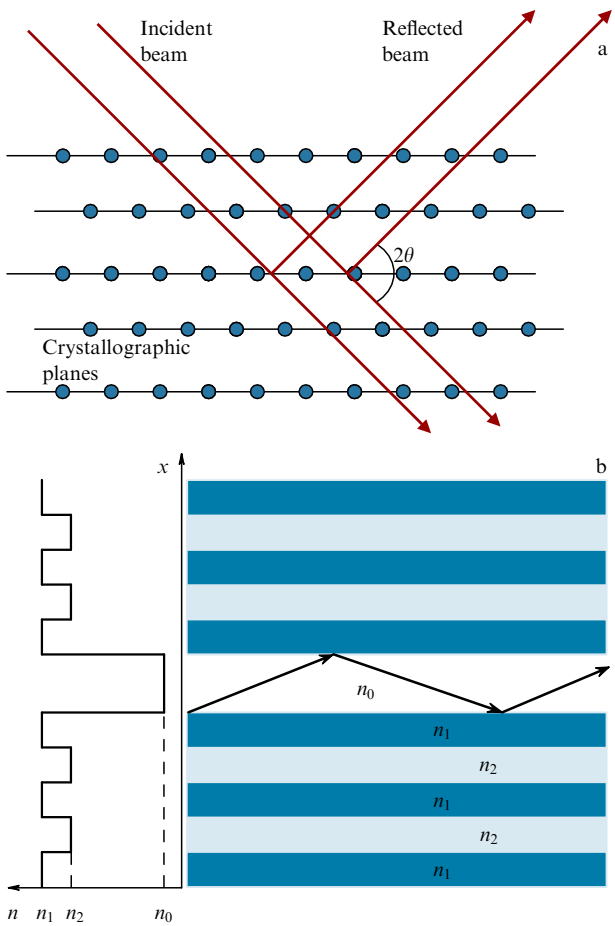

Figure 2. Bragg diffraction of X-rays from a crystal lattice (a) and guided modes of laser radiation in a waveguide with a periodic cladding (b).

on the order of the optical wavelength are called photonic crystals [59–62]. Frequency ranges where the forward and reflected waves of electromagnetic radiation are strongly coupled in photonic crystals are referred to as photonic band gaps. The high reflectivity of photonic-crystal structures within PBGs can be employed to confine guided modes of electromagnetic field to an area of low refractive index (Fig. 2b), i.e., to achieve low-loss waveguiding with a relation between the refractive indices of the core and the cladding opposite the one required for total internal reflection. The possibility of guiding light in a layer sandwiched between materials with higher refractive indices was first experimentally demonstrated for planar waveguides with a periodic cladding (Fig. 2b) by Yariv's group [63]. Optical fibers based on this idea — hollow-core photonic-crystal fibers — were first developed and demonstrated by Russell's group [41] in 1999 (see references [42–45] for an up-to-date review of hollow PCFs).

Thus, the idea of reducing optical losses in a hollow waveguide with a periodic cladding relative to a hollow waveguide with a solid cladding is based on the high reflectivity of a periodic structure within PBGs. To illustrate this idea, we employ a geometric-optic approach to the analysis of guided modes (Fig. 2b). Physically, optical losses originate from the reflection of radiation from waveguide walls. The attenuation coefficient α can then be found from the following relation [64]:

$$R^{2M} = \exp(-\alpha L)\,, \tag{1}$$

where R is the reflection coefficient and M is the number of reflections from waveguide walls per length L.

For a waveguiding layer (a fiber core) with a size a, the number of reflections M is given by

$$M = \frac{L}{2a\tan\theta}\,. \tag{2}$$

Here, θ is the angle of incidence, which can be expressed in terms of the propagation constant K and its transverse part h as

$$h\tan\theta = K\,. \tag{3}$$

Formulas (1)–(3) yield the following expression for the attenuation coefficient:

$$\alpha = -\frac{h}{aK}\ln R\,. \tag{4}$$

The reflection coefficient R in our case is determined by standard Fresnel formulas. For TE waves making small angles θ with the waveguide walls, we derive [21]

$$\alpha_h^l = \frac{l^2\lambda^2}{n_1 a^3 (n_2^2 - n_1^2)^{1/2}}\,, \tag{5}$$

where n_1 and n_2 are the refractive indices of the waveguiding layer and the cladding, respectively, and l is an integer corresponding to the mode index.

Thus, we find that the magnitude of optical losses in our system scales as λ^2/a^3, which is typical of hollow waveguides. This scaling law often prevents one from using long hollow waveguides when a small core size is necessary to achieve a high power density of laser radiation.

This conflict is resolved in a hollow waveguide with a periodic cladding. Suppose that the refractive index of the waveguiding layer is equal, as before, to n_1, but the cladding now consists of alternating layers with refractive indices n_1 and n_2. The coefficient of reflection from the waveguide walls can then be written as [64]

$$R_{\rm PBG} = \frac{-{\rm i}\varkappa^*\sinh(sNd)}{s\cosh(sNd) + {\rm i}(\Delta\beta/2)\sinh(sNd)}\,, \tag{6}$$

where

$$s^2 = \varkappa^*\varkappa - \left(\frac{\Delta\beta}{2}\right)^2, \tag{7}$$

$$\Delta\beta = 2\bar{n}\,\frac{\omega}{c}\cos\theta - \frac{2\pi m}{d} = 2\,\frac{\bar{n}}{c}\cos\theta(\omega - \omega_0) \tag{8}$$

is the detuning from the Bragg resonance for a periodic structure of the waveguide cladding with a period d, ω_0 is the central frequency of the photonic band gap of the cladding, $\bar{n} = [(n_1^2 + n_2^2)/2]^{1/2}$, m is an integer, d is the modulation period of the refractive index in the cladding, N is the number of periods in the waveguide cladding, and $\varkappa$ is the coefficient of coupling of forward and backward waves in the periodic cladding. For a TE wave with $m = 1$, this coupling coefficient is [64]

$$\varkappa = \frac{\sqrt{2}{\rm i}(n_2^2 - n_1^2)}{\lambda\cos\theta(n_2^2 + n_1^2)^{1/2}}\,. \tag{9}$$

Around the center of the photonic band gap, where $|\Delta\beta| \ll |\varkappa|$, we have

$$R_{\rm PBG} = \tanh\left(|\varkappa|Nd\right). \tag{10}$$

The ratio of the magnitude of optical losses in a hollow waveguide with a periodic cladding to the magnitude of optical losses in a hollow waveguide with a solid cladding is thus controlled by the ratio of the logarithms of the coefficients of reflection from the waveguide walls. For sufficiently large arguments of the hyperbolic tangent in Eqn (10), we find that

$$\frac{\alpha_{\rm PBG}}{\alpha_h} \propto a\exp\left(-2|\varkappa|Nd\right). \tag{11}$$

Hence, the increase in the number of periods in the cladding of a hollow waveguide leads to an exponential decrease in the optical losses of waveguide modes relative to the optical losses in a conventional, solid-cladding hollow waveguide.

Within the framework of the geometric-optic approach, the propagation constant $K_{\rm PBG}$ of modes in a hollow waveguide with a periodic cladding is given by

$$K_{\rm PBG}^2 = \left(\frac{\omega}{c}\right)^2 n_1^2 - h^2\,, \tag{12}$$

$$ah = \pi q + 2\varphi\,, \tag{13}$$

where q is an integer and φ is the phase shift per single reflection from a waveguide wall.

Using Eqn (6) for the coefficient of reflection from a periodic multilayer, we arrive at

$$ah = \pi q + 2\arctan\left[\frac{\Delta\beta}{2s}\tanh(sNd)\right]. \tag{14}$$

Close to the center of a PBG, Eqn (14) yields an expression similar to the formula for the propagation constants of guided

modes in a hollow waveguide with a solid cladding:

$$K_{\mathrm{PBG}}^{q} \approx \frac{\omega}{c}\, n_1 \left[1 - \frac{(\pi q c)^2}{(a\omega n_1)^2}\right]^{1/2}. \qquad (15)$$

As can be seen from Eqn (15), a hollow waveguide with a periodic cladding, similar to a standard, solid-cladding hollow waveguide, can phase-match frequency-nondegenerate nonlinear-optical interactions, but provide much higher levels of signal transmission as compared to standard hollow waveguides. The structure of cladding in realistic hollow PCFs is much more complicated than the periodic multilayer stack considered in this section. Analysis of guided modes in hollow PCFs generally requires a numerical solution of the relevant wave equations. Such a treatment will be provided in the following section.

3. Waveguide modes of hollow-core photonic-crystal fibers

In this section, we will examine the spatial distribution of the electromagnetic field in air-guided modes of hollow PCFs and investigate dispersion properties of such modes. For this analysis, we will employ the numerical solution of the wave equation for the electromagnetic field in a hollow PCF [65] performed by using the method of field expansion in Hermite – Gauss polynomials, originally developed in [66 – 68].

Waveguide modes and transmission spectra of hollow PCFs are modeled by numerically solving the vectorial wave equations for the transverse components of the electric field $E_x(x, y)$ and $E_y(x, y)$:

$$\left[\frac{\nabla_\perp^2}{k^2} + n^2(x,y)\right] E_x + \frac{1}{k^2}\frac{\partial}{\partial x}\left(E_x \frac{\partial \ln n^2}{\partial x} + E_y \frac{\partial \ln n^2}{\partial y}\right) = \frac{\beta^2}{k^2} E_x\,, \qquad (16)$$

$$\left[\frac{\nabla_\perp^2}{k^2} + n^2(x,y)\right] E_y + \frac{1}{k^2}\frac{\partial}{\partial y}\left(E_x \frac{\partial \ln n^2}{\partial x} + E_y \frac{\partial \ln n^2}{\partial y}\right) = \frac{\beta^2}{k^2} E_y\,, \qquad (17)$$

where β is the propagation constant, k is the wave number, $\nabla_\perp$ is the gradient in the (x, y) plane, and $n(x, y)$ is the spatial profile of the refractive index.

The transverse distribution of the electric field in the PCF cross section is represented as a series expansion in a set of orthonormalized Hermite – Gauss polynomials:

$$E_x = \sum_{n,m=0}^{F-1} \xi_{n,m}^{x}\, \psi_n\left(\frac{x}{\Lambda}\right)\psi_m\left(\frac{y}{\Lambda}\right),$$

$$E_y = \sum_{n,m=0}^{F-1} \xi_{n,m}^{y}\, \psi_n\left(\frac{x}{\Lambda}\right)\psi_m\left(\frac{y}{\Lambda}\right). \qquad (18)$$

The profile of the refractive index is expanded in Hermite – Gauss polynomials and a set of orthogonal periodic functions:

$$n^2(x,y) = \sum_{n,m=0}^{N_d-1}\left[D_{n,m}\,\psi_n\left(\frac{x}{w}\right)\psi_m\left(\frac{y}{w}\right)\right] + \sum_{k,l}^{N_p-1} P_{k,l}\cos\frac{2\pi k x}{T_x}\cos\frac{2\pi l y}{T_y}\,, \qquad (19)$$

where N_d and N_p are the dimensions of the basis of expansion functions; $D_{n,m}$ and $P_{k,l}$ are constant coefficients; T_x and T_y are the periods of the structure of the PCF cladding along the x- and y-axes, respectively; and Λ and w are the spatial scales of the PCF cross section. Dispersion properties of guided modes in a hollow PCF were calculated using series expansions in a basis of 80×80 Hermite – Gauss polynomials and 150×150 trigonometric functions. Figure 3 displays a one-dimensional cut (Fig. 3a) and a two-dimensional profile (Fig. 3b) of the refractive index squared synthesized with Eqn (19).

Substitution of series expansions (18) and (19) into wave equations (16) and (17) reduces the initial problem to an eigenfunction and eigenvalue problem of a matrix equation, which allows the propagation constants (Fig. 4a), group-velocity dispersion (GVD) (Fig. 4b), and transverse field profiles (Fig. 5) to be determined for the air-guided modes of hollow PCFs. Simulated two-dimensional field intensity profiles in the fundamental and higher order PCF modes (Figs 5a, c, e, g) agree well with the results of experiments [46, 69] performed with air-filled hollow PCFs having a core diameter of about 14 μm and a glass – air periodic cladding with a period of about 5 μm (Figs 5b, d, f, h).

Experimental data [46, 69] and results of simulations [65] indicate the possibility of excitation of the fundamental and several isolated higher order air-guided modes confined to the hollow core of the PCF. The number of guided modes supported by the hollow core of a PCF is controlled by the width of the PBG of the PCF cladding and the ratio of the

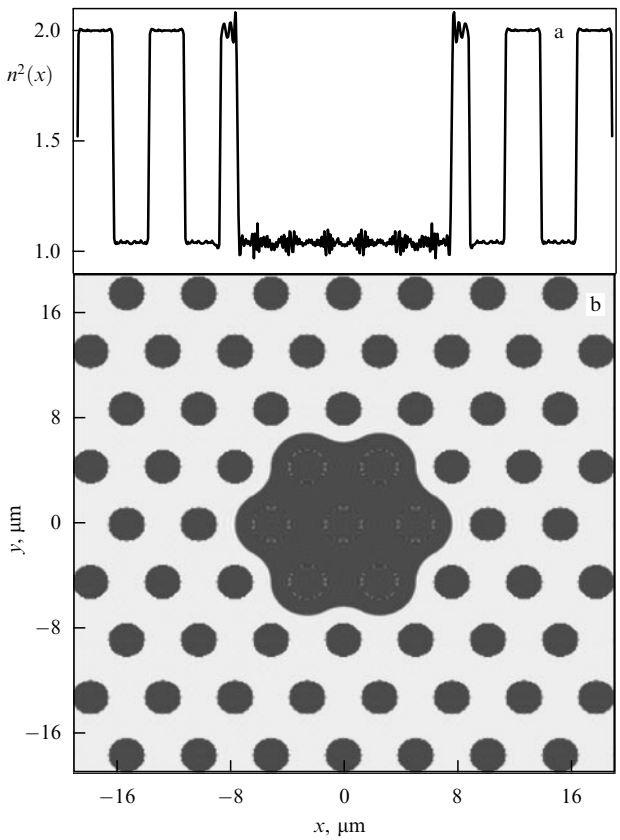

Figure 3. One-dimensional cut of the refractive-index profile along the x-axis at $y = 0$ (a) and the profile of the refractive index squared in the cross section of the hollow PCF (b) synthesized by polynomial expansion ($N_d = 80$, $N_p = 150$).

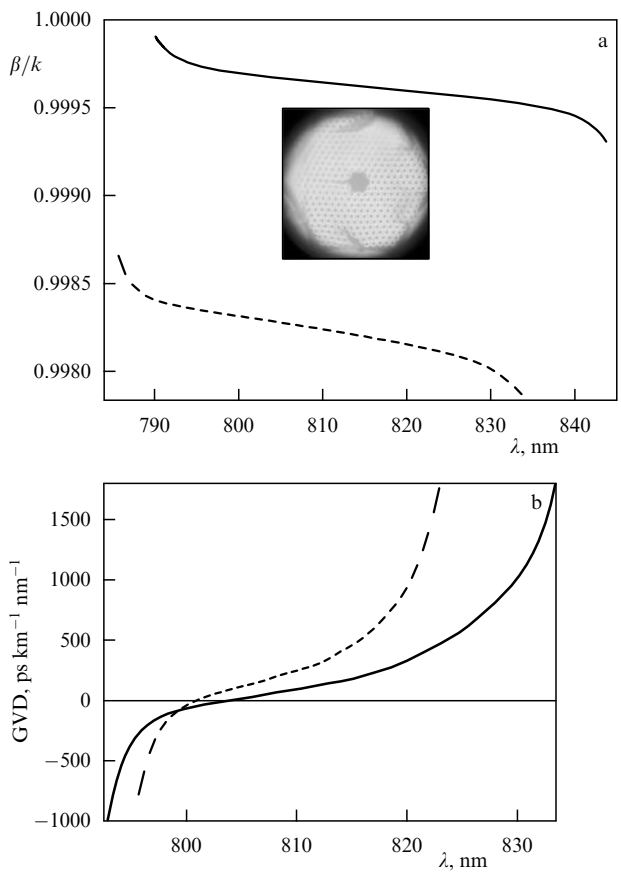

Figure 4. Propagation constant β normalized to the wave number k (a) and group-velocity dispersion (b) as functions of the wavelength for the fundamental (solid curve) and the second-order (dashed curve) air-guided modes of a hollow PCF with the cross-section structure shown in the inset.

PCF core radius r_{core} to the radiation wavelength. An intuitive estimate of the number of air-guided modes in a PCF is provided by an approximate formula proposed by Cregan et al. [41]:

$$N_{\text{PCF}} = \frac{1}{4}(\beta_{\text{h}}^2 - \beta_{\text{l}}^2)\, r_{\text{core}}^2 \,, \tag{20}$$

where β_{h} and β_{l} are the propagation constants at the upper and lower edges of the respective PBG of the cladding.

Formula (20) gives a physically instructive approximation of the number and density of air-guided modes in a hollow PCF, which generally agrees quite well on the qualitative level with the results of more accurate numerical simulations [70]. This formula shows, in particular, that PBGs of the photonic-crystal cladding not only serve to lower propagation losses of air-guided modes relative to a conventional, solid-cladding hollow fiber with the same core diameter, but also filter air-guided modes, facilitating a selective preparation and addressing of isolated waveguide modes of the electromagnetic radiation field.

It can also be seen from Eqn (20) that the number of air-guided modes of a PCF increases with the growth in the ratio of the core radius to the radiation wavelength. Figure 6 displays a cross-section image of a hollow PCF with a large core area, designed [71] for the transmission of high-intensity laser pulses. This fiber can generally support multimode waveguiding regimes. With an appropriate input beam coupling geometry, however, selective excitation of isolated air-guided modes becomes possible, facilitated by the filtering effect of PBGs of the PCF cladding. In the short-wavelength regime ($\lambda \ll r_{\text{core}}$), the fiber is essentially multimode. Typical field intensity profiles for high-order air-guided modes of this fiber are presented in Fig. 7.

Both passbands in PCF transmission and dispersion properties of air-guided modes in these fibers can be tuned by changing the fiber structure [69]. Group-velocity dispersion,

$$D = -2\pi c \lambda^{-2} \frac{\mathrm{d}^2\beta}{\mathrm{d}\omega^2}$$

is the key parameter of a fiber that governs the spreading of short laser pulses propagating through a fiber. Negative GVD

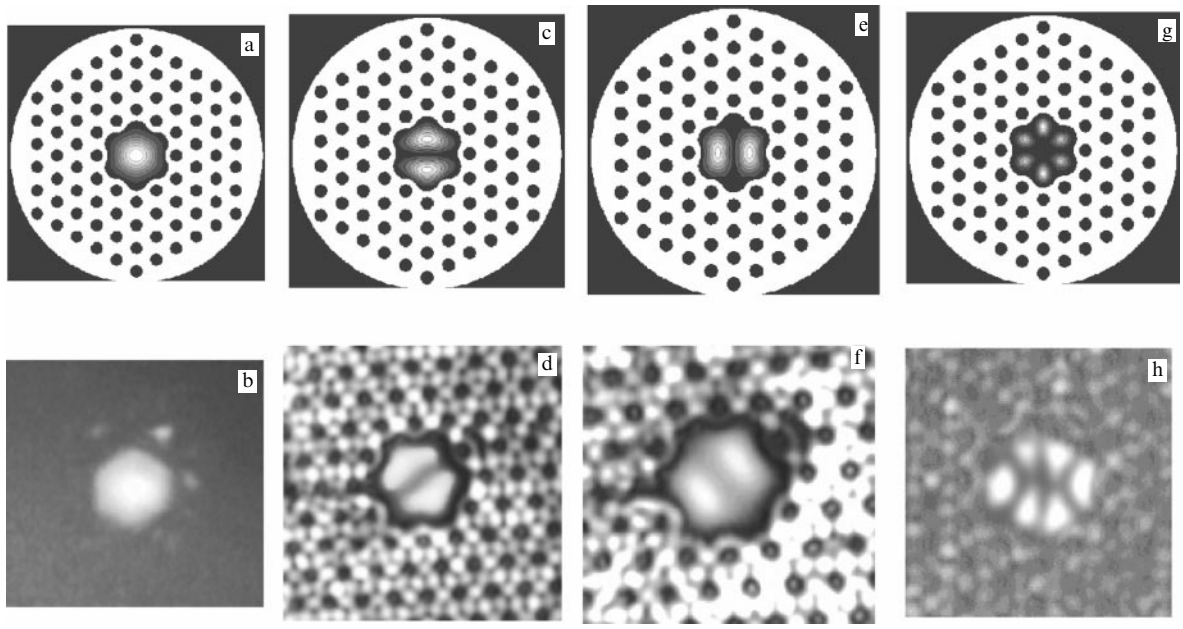

Figure 5. Results of simulations (a, c, e, g) and experiments (b, d, f, h) for field-intensity profiles in air-guided modes of a hollow PCF.

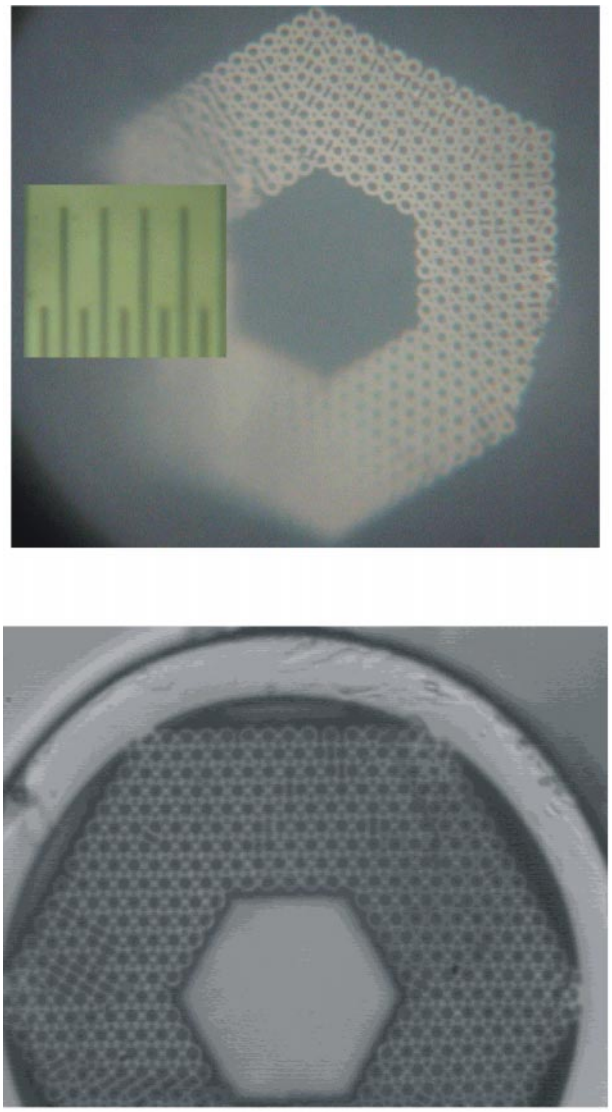

Figure 6. Cross-section images of large-core-area hollow photonic-crystal fibers (with a core radius of about 23 μm) designed to transmit high-intensity laser pulses (the lower image shows the field-intensity profile in the guided mode). The main division of the ruler on the left-hand side of the top image corresponds to 10 μm.

corresponds to normal dispersion, while areas of positive GVD are referred to as ranges of anomalous dispersion. Figure 4b presents the group-velocity dispersion for the fundamental and higher order modes of the hollow PCF with the cross-section structure shown in the inset in Fig. 4a.

As can be seen from the results presented in Fig. 4b, group-velocity dispersion of PCF modes may substantially exceed in its absolute value the GVD of both bulk fused silica and air. The GVD becomes especially strong close to the edges of the passbands in PCF transmission. This observation is consistent with the results of earlier experimental studies on the propagation of femtosecond pulses in hollow PCFs [72, 73]. Quite typically, the GVD vanishes in the central part of the passband, becoming anomalous within a rather broad frequency range, which can be employed for the generation of solitons [51, 52] or the self-compression of ultrashort laser pulses.

4. Nonlinear-optical interactions of isolated air-guided modes of high-intensity femtosecond laser pulses

Nonlinear optics of high-intensity ultrashort laser pulses is one of the most interesting and rapidly growing areas of optical physics. Nonlinear-optical interactions of high-intensity femtosecond laser pulses are at the heart of several new physical phenomena, including high-order harmonic generation [74, 75], and allow unprecedentedly short, attosecond pulses to be synthesized [76 – 78]. Hollow PCFs implement new waveguide regimes for high-intensity ultrashort laser pulses, offering unique options for strong-field optics. In particular, such fibers can support air-guided modes of electromagnetic radiation with transverse sizes of only a few micrometers, providing a radical enhancement of nonlinear-optical interactions of ultrashort laser pulses [47 – 49, 79].

Figure 8 displays transmission spectra of hollow PCFs [73] designed for a waveguide transportation of femtosecond Ti: sapphire-laser pulses (Fig. 8a), as well as the fundamental radiation of an Nd : YAG laser and its second harmonic (Fig. 8b). The hollow PCF with the transmission spectrum presented in Fig. 8c is designed to guide infrared radiation within the range of wavelengths from 1.0 to 1.25 μm and from 1.6 to 2.0 μm. The fibers employed in experiments [73] had a photonic-crystal cladding with a period of 5 μm and a core diameter of 14 μm. A typical cross-section view of the PCF is presented in the inset in Fig. 8a.

Transmission spectra of hollow-core PCFs display characteristic well-pronounced isolated peaks (Fig. 8). The origin of these peaks, as mentioned above, is associated with the

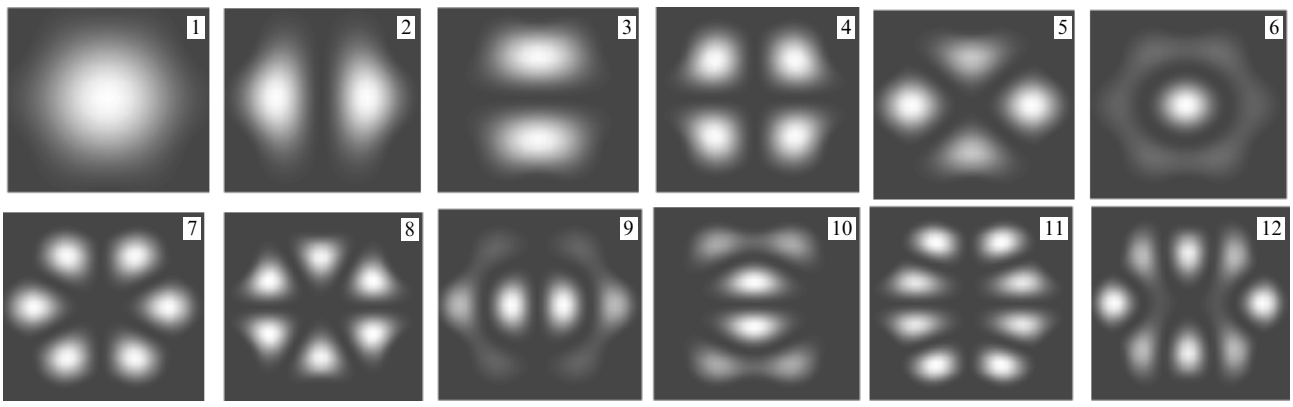

Figure 7. Field-intensity profiles in the guided modes of a hollow PCF simulated by the method of polynomial expansion.

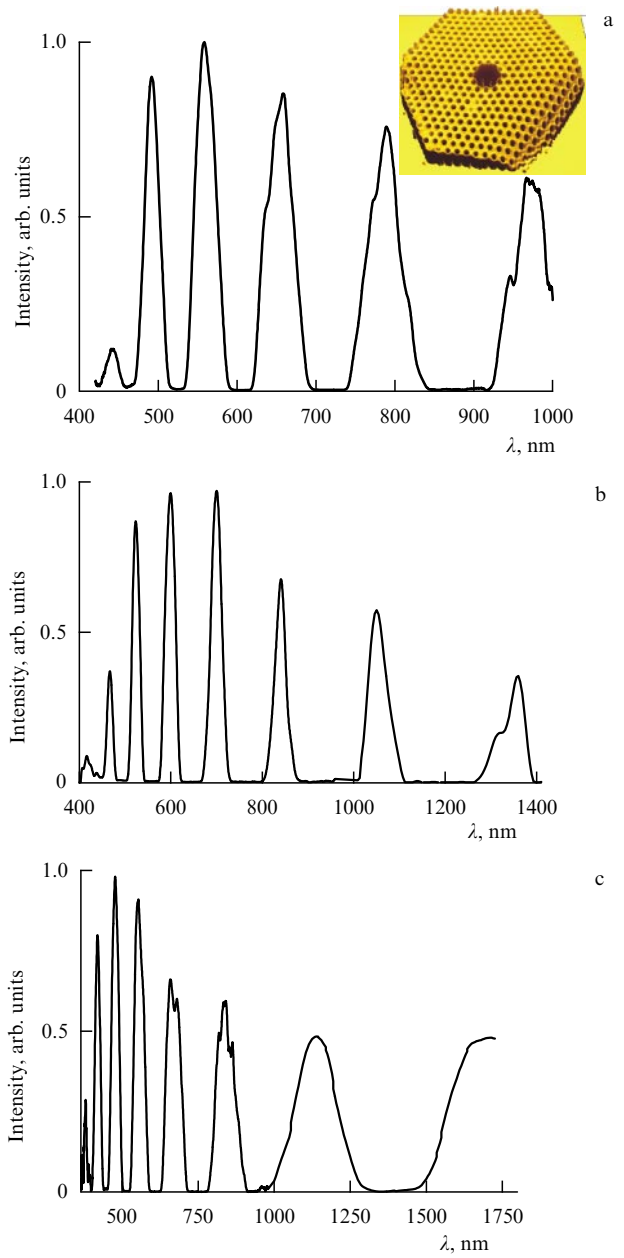

Figure 8. Transmission spectra of hollow-core PCFs designed to transmit femtosecond pulses of Ti:sapphire-laser radiation (a), the fundamental radiation of an Nd:YAG laser and its second harmonic (b), and infrared radiation within the range of wavelengths from 1.0 to 1.25 μm and from 1.6 to 2.0 μm (c). The inset in Fig. 8a shows the cross-section image of the hollow PCF with a period of the cladding equal to 5 μm and a core diameter of about 13 μm.

high reflectivity of a periodically structured fiber cladding within photonic band gaps, which substantially reduces radiation losses in guided modes within narrow spectral ranges. Radiation with wavelengths lying outside the photonic band gaps of the cladding leaks from the hollow core. Such leaky radiation modes are characterized by high losses, giving virtually no contribution to the signal at the output of the fiber. The spectra of air-guided modes in hollow-core PCFs can be tuned by changing the fiber cladding structure [69]. Waveguide modes of hollow PCFs and their transmission spectra were modeled by solving vectorial wave equations for the electric field using the numerical procedure developed in [65, 69] and described in Section 3 of this review.

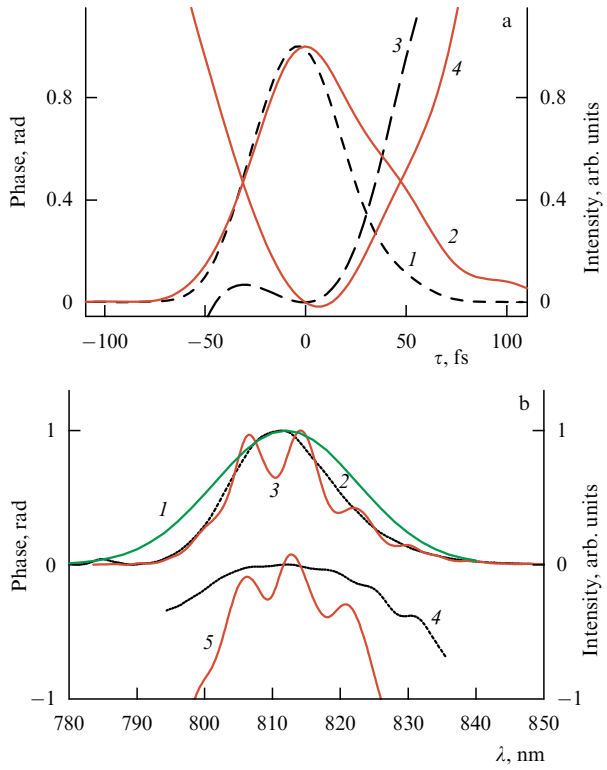

Figure 9. (a) The envelope (*1*, *2*) and the chirp (*3*, *4*) of a Ti: sapphire-laser pulse transmitted through a 3-cm hollow-core photonic-crystal fiber with the structure of the cross section shown in the inset in Fig. 4a (solid lines) and a pulse at the output of the Ti:sapphire laser (dashed lines). (b) Evolution of the spectrum and the spectral phase of a Ti: sapphire-laser pulse transmitted through a hollow-core photonic-crystal fiber: (*1*) the passband of the PCF, (*2*) the initial spectrum of the pulse, (*3*) the spectrum of the pulse transmitted through a 3-cm PCF, (*4*) the initial spectral phase of the pulse, and (*5*) the spectral phase of the pulse transmitted through a 3-cm PCF. The wavelength of laser radiation is 812 nm.

The envelope and phase evolution of ultrashort laser pulses guided through optical fibers may noticeably influence the propagation regime and the efficiency of nonlinear-optical interactions of ultrashort laser pulses, eventually determining the possibility of subsequent spectral and temporal transformations of laser pulses. Konorov et al. [73] have experimentally studied changes in the envelope, as well as the evolution of the spectral phase and the chirp of femtosecond pulses transmitted through hollow PCFs.

The results of these experiments (Fig. 9) indicate that envelope and phase distortions of ultrashort pulses guided through hollow PCFs are controlled by the detuning of the carrier frequency of laser pulses from the central frequency of the PCF passband. Distortions of the pulse envelope, as well as time- and frequency-dependent phase shifts become especially noticeable (Fig. 9) around the edges of PCF passbands, corresponding to the edges of the photonic band gaps of the fiber cladding. Away from the edges of these PBGs, hollow PCFs can provide optimal conditions for the transmission of ultrashort pulses. However, waveguide dispersion effects near the edges of PCF transmission passbands may play a noticeable role, especially in hollow PCFs with a small core diameter, leading to considerable distortions in the envelope, chirp, and the spectral phase of ultrashort pulses.

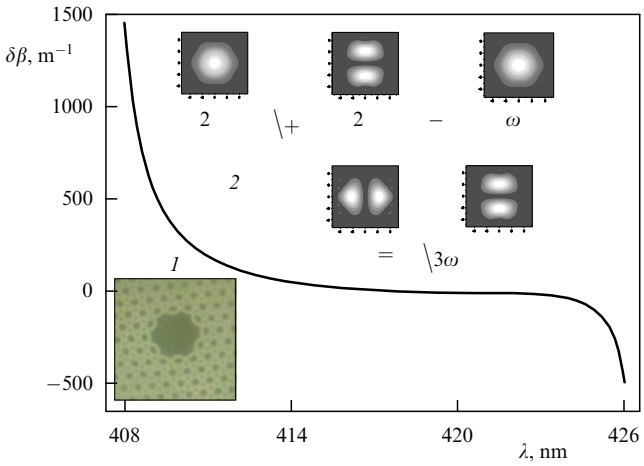

Figure 10. The mismatch $\delta\beta = \beta_{3\omega} - \beta'_{2\omega} - \beta''_{2\omega} + \beta_{\omega}$ of the propagation constants β_{ω}, $\beta'_{2\omega}$, $\beta''_{2\omega}$, and $\beta_{3\omega}$ of air-guided modes involved in the four-wave mixing $3\omega = 2\omega + 2\omega - \omega$ (2ω and ω are the frequencies of the pump fields) in a hollow PCF with a period of photonic-crystal cladding equal to 4.6 μm and a core diameter of approximately 13 μm. The insets show (*1*) an image of the PCF cross section and (*2*) field-intensity profiles for the air-guided modes of the hollow PCF involved in the FWM process.

As shown in [80], hollow-core PCFs with a special dispersion profile can phase-match nonlinear-optical interactions of isolated air-guided modes of high-intensity femtosecond laser pulses confined in the hollow fiber core. Hollow-core PCFs designed for the purposes of these experiments had a period of photonic-crystal cladding of about 4.6 μm and a core diameter of approximately 13 μm. A typical structure of the PCF cross section is shown in inset *1* in Fig. 10. Figure 10 displays the mismatch

$$\delta\beta = \beta_{3\omega} - \beta'_{2\omega} - \beta''_{2\omega} + \beta_{\omega}$$

of the propagation constants β_{ω}, $\beta'_{2\omega}$, $\beta''_{2\omega}$, and $\beta_{3\omega}$ of air-guided modes in the PCF involved in the FWM process

$$3\omega = 2\omega + 2\omega - \omega$$

(2ω and ω are the frequencies of the pump fields). The results presented in this plot indicate a nearly perfect phase matching for the FWM of the fundamental mode of fundamental radiation ω of a Cr:forsterite laser, the fundamental mode of one of the second-harmonic fields 2ω, a higher order guided mode of the other second-harmonic field 2ω, and a higher guided mode of the nonlinear signal (see inset *2* in Fig. 10). The phase matching, as can be seen from Fig. 10, is achieved within a spectral range with a bandwidth of about 10 nm, allowing a highly efficient FWM of broadband, femtosecond laser pulses. The experimental results presented below are fully consistent with this theoretical analysis.

The laser system employed in experiments [80] consisted of a Cr^{4+}: forsterite master oscillator, a stretcher, an optical isolator, a regenerative amplifier, a compressor, and a crystal for frequency doubling (Fig. 11). The master oscillator, pumped with a fiber ytterbium laser, generated 30 – 50-fs light pulses with a repetition rate of 120 MHz, a central wavelength of 1250 nm, and a mean power of about 180 mW. These pulses were then transmitted through a stretcher and an isolator to be amplified in an Nd: YLF-laser-pumped amplifier. Amplified pulses with an energy up to 100 μJ were recompressed to a 50 – 100-fs pulse duration in a grating compressor. Approximately 50% of the radiation energy was lost at this stage. An LBO crystal was used to generate the second harmonic of amplified Cr:forsterite-laser radiation.

Femtosecond pulses of 1250-nm fundamental radiation and 625-nm second-harmonic radiation of the Cr:forsterite laser with pulse energies ranging from 0.1 up to 10 μJ were used as pump fields ω and 2ω in the FWM process $3\omega = 2\omega + 2\omega - \omega$. These pulses were coupled into a 5-cm hollow PCF with a period of cladding equal to 4.6 μm and a core diameter of about 13 μm, placed on a three-dimensional translation stage, with a standard micro-objective. Fundamental radiation was focused in such a way as to provide the maximum efficiency of beam coupling into the fundamental mode of the PCF (inset *1* in Fig. 12). The second harmonic was coupled into a mixture of the fundamental and higher order air-guided modes (inset *2* in Fig. 12).

The FWM of these two pump fields induced by the third-order nonlinearity of the atmospheric-pressure air filling the PCF resulted in the generation of a signal with a central wavelength of 417 nm (Fig. 12). The maximum efficiency of FWM frequency conversion was estimated as 0.1%. Because of poor phase matching, direct third-harmonic generation $3\omega = \omega + \omega + \omega$, giving rise to a nonlinear signal with the

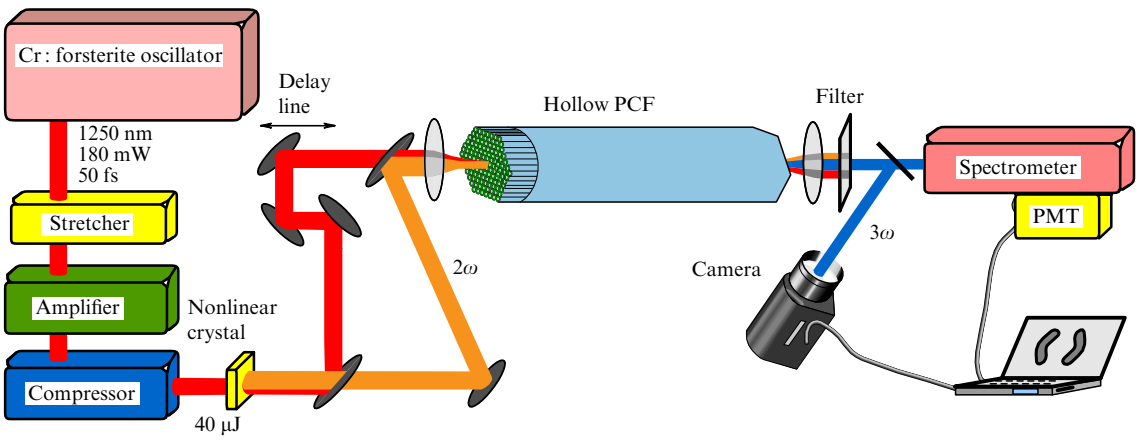

Figure 11. Diagram of the femtosecond laser system for the investigation of nonlinear-optical interactions of high-intensity ultrashort laser pulses in a hollow photonic-crystal fiber.

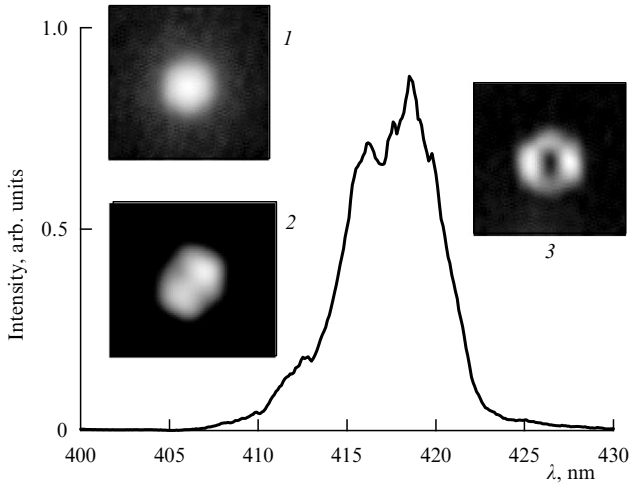

Figure 12. The spectrum of the FWM signal generated in the hollow photonic-crystal fiber by the pulses of fundamental radiation and the second harmonic of the Cr:forsterite laser with input energies of 2 and 3 μJ, respectively. The initial duration of the pump pulses of fundamental radiation is about 50 fs. The insets show the spatial field-intensity profiles measured for the fundamental (*1*) and second-harmonic (*2*) pump beams and the FWM signal (*3*) at the output of the PCF.

same central wavelength, was several orders of magnitude less efficient than the two-color FWM $3\omega = 2\omega + 2\omega - \omega$.

Analysis of the transverse intensity profile of the FWM signal at the output of the hollow PCF shows that the nonlinear signal is generated in a stable isolated well-resolved higher order air-guided mode of the PCF (inset *3* in Fig. 12). This finding agrees well with the theoretical analysis of phase matching for the considered FWM process in the hollow PCF (cf. inset *2* in Fig. 10 and insets *1 – 3* in Fig. 12). We can argue, therefore, that the spatial beam profile of the FWM signal generated in a PCF as a result of nonlinear-optical interaction of isolated air-guided modes of pump radiation is dictated and stabilized by phase-matching conditions. This remarkable property of FWM in a hollow PCF provides a high beam quality of the nonlinear signal at the output of the fiber and suggests an exciting opportunity for mode-controlled nonlinear-optical processing of high-intensity laser pulses.

The spatial beam profile of the FWM signal at the output of the PCF remained stable up to the energy of input pump pulses of about 6 μJ, corresponding to a light-field intensity of about 9×10^{13} W cm^{-2}. Spatial self-action and ionization effects started to play a noticeable role above this level of input laser intensities, leading to instabilities and distortions in output beam profiles of the pump and FWM fields. Laser pulses with energies exceeding 10 μJ caused optical damage on the PCF inner walls, resulting in an irreversible degradation of fiber transmission and a substantial lowering of the FWM efficiency.

Tailored dispersion of air-guided modes in hollow PCFs offers new phase-matching solutions not only for four-wave mixing, but also for nonlinear-optical processes of higher orders. In particular, Serebryannikov et al. [81] have demonstrated the possibility of using hollow PCFs for phase-matched high-order harmonic generation. Hollow fibers radically enhance this process due to the large length of nonlinear-optical interaction provided in the waveguide regime. Hollow PCFs suggest ways toward highly efficient harmonic generation in field of pulses with a moderate power through multiwave nonlinear-optical interactions of air-guided modes of electromagnetic radiation with controlled transverse intensity profiles.

Figure 13 illustrates phase matching for the generation of high-order harmonics of the pump field with a wavelength of 800 nm, giving rise to harmonic emission within the range of wavelengths from 25 up to 45 nm. The phase-matching condition requires the equality of the effective refractive indices $n_{\rm eff} = \beta c/\omega$ for the PCF-guided modes of the pump and harmonic fields. Exact phase matching for high-order harmonic generation in hollow PCFs is achieved through the appropriate choice of optimal gas pressure (Fig. 13a), as well as fiber structure and type of modes involved in the nonlinear-optical interaction (Fig. 13b).

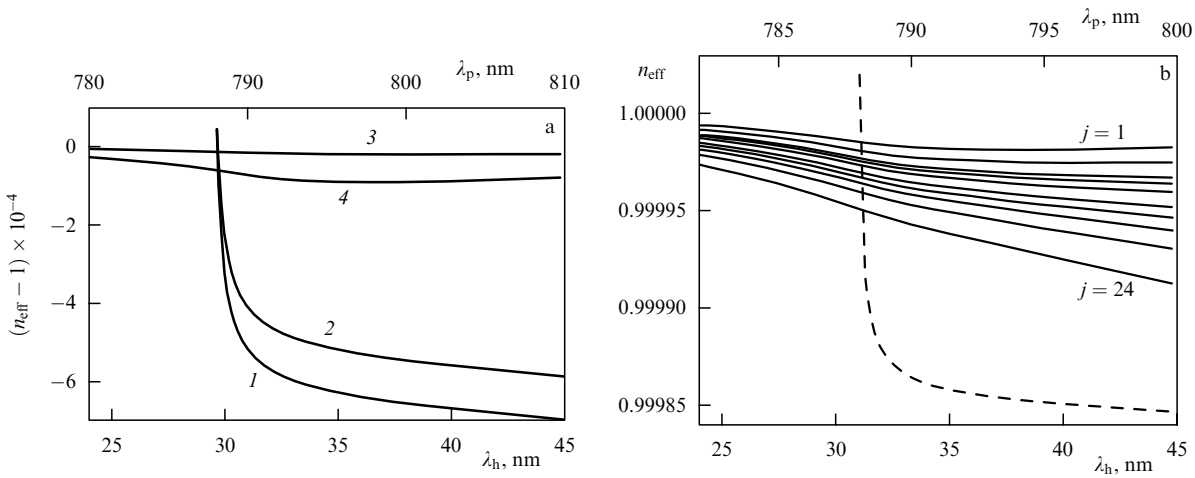

Figure 13. (a) Effective refractive indices for the fundamental modes of the pump field (*1*, *2*) and high-order harmonics (*3*, *4*) calculated as functions of the pump and harmonic wavelengths $\lambda_{\rm p}$ and $\lambda_{\rm h}$ for a hollow PCF with a period of cladding equal to 5 μm filled with argon at a pressure of 0.1 atm (*1*, *3*) and 0.5 atm (*2*, *4*). (b) Effective refractive indices for the fundamental mode of the pump field (the dashed line) and the fundamental ($j = 1$) and higher order ($j = 2 – 13$, 18, 24) modes of high-order harmonics calculated as functions of the pump and harmonic wavelengths $\lambda_{\rm p}$ and $\lambda_{\rm h}$ for a hollow PCF with a period of cladding equal to 10 μm filled with argon at a pressure of 0.1 atm. Field-intensity profiles in high-order modes of hollow PCFs are shown in Fig. 7.

The results of experimental and theoretical studies presented in this section show that hollow-core PCFs with a special dispersion profile allow phase-matched nonlinear-optical interactions of isolated air-guided modes of high-intensity femtosecond laser pulses confined in the hollow fiber core. Phase matching of isolated air-guided modes of high-intensity femtosecond laser pulses involved in nonlinear-optical interactions in a hollow PCF provides a high efficiency of frequency conversion for ultrashort laser pulses with an intensity on the order of 10^{14} W cm^{-2} and stabilizes the spatial intensity profile of the output FWM signal.

5. Self-action of subgigawatt femtosecond pulses

In this section, we will discuss the results of experiments devoted to the investigation of temporal and spatial self-action of high-power (subgigawatt) femtosecond laser pulses in hollow PCFs. We will explore ways of optimizing hollow PCFs for the transportation of high-power laser pulses and demonstrate the possibility of using Kerr-nonlinearity-induced self-focusing in such waveguides for the transmission of laser radiation in the regime of self-channeling.

Because of the finite bandwidth of the photonic band gaps of the PCF cladding, the width of passbands in PCF transmission is also finite (Fig. 8). This circumstance, on the one hand, limits the duration of pulses that can be transmitted through such fibers, allowing, on the other hand, creation of optical diodes [50], as well as limiters and switches [82] for high-intensity ultrashort laser pulses based on self-phase modulation in hollow PCFs.

Temporal and spatial self-action of laser pulses in hollow PCFs was studied [83] by using radiation of a Ti:sapphire laser system consisting of a master oscillator and a regenerative amplifier. The central wavelength of laser pulses was approximately 800 nm, with their duration being about 30 fs and energy ranging from 0.1 up to 10 μJ. A standard micro-objective was used to couple laser pulses into the hollow core of a PCF placed on a three-coordinate translation stage inside a vacuum chamber. Experimental studies of temporal and spatial self-action of laser pulses were performed with PCFs filled with argon, nitrogen, and atmospheric air within the range of pressures from 0.1 up to 10 atm.

Transmission of ultrashort pulses through hollow PCFs with minimal losses requires matching the spectrum of the laser pulses with the transmission spectrum of the PCF. The width of a passband in the transmission spectrum of a hollow PCF, controlled by the photonic band gap of the cladding, should be sufficient for the transmission of ultrashort laser pulses spectrally broadened due to self-phase modulation without considerable distortions in the pulse envelope.

Figure 14 presents the spectra of radiation coming out of a 6-cm PCF filled with nitrogen (Fig. 14a) and argon (Figs 14b, c) at different pressures. The initial energy of femtosecond Ti:sapphire-laser pulses coupled into the PCF was about 0.2 μJ. The spectra of output pulses are broadened with respect to the input pulses due to self-phase modulation. Optimal conditions for the transmission of spectrally broadened pulses through the PCF are achieved when the spectrum of the pulse is matched with the relevant passband in the transmission of the PCF. Figure 14a shows an example of such optimal matching. The bandwidths of SPM-broadened pulses presented in Figs 14b and 14c exceed the width of the PCF passband, which gives rise to additional radiation losses.

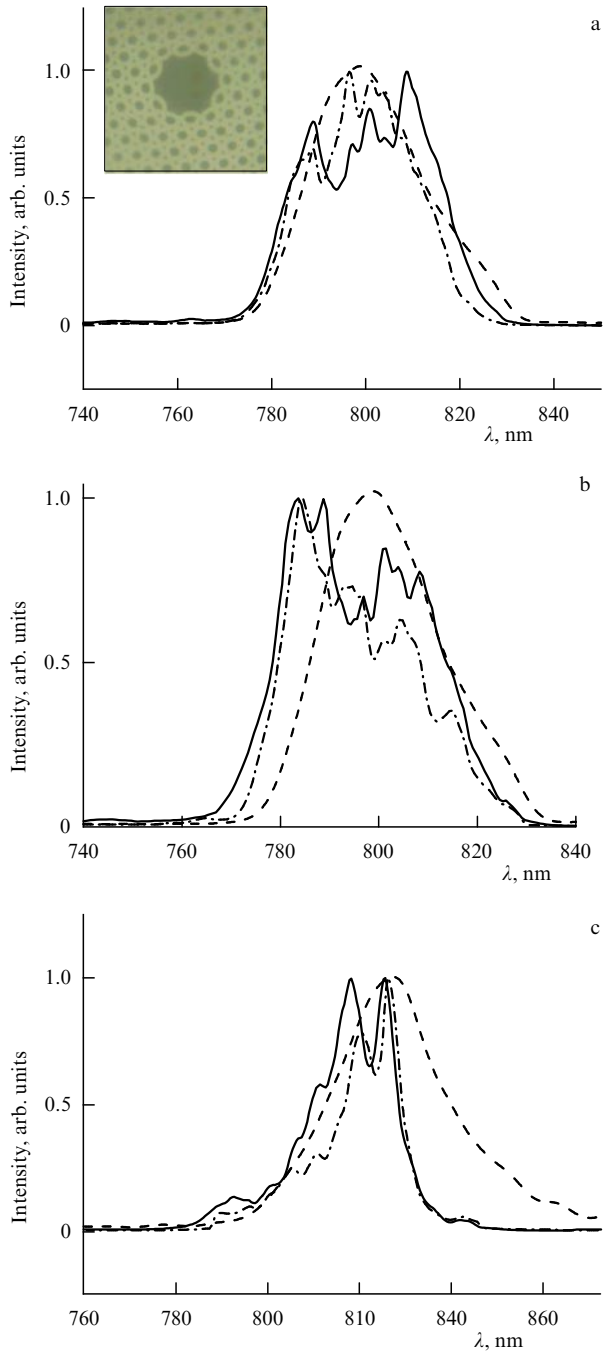

Figure 14. Spectra of ultrashort laser pulses broadened by self-phase modulation in hollow photonic-crystal fibers filled with (a) nitrogen and (b, c) argon at a pressure of 3 atm (dash – dotted line) and 5 atm (solid line). The fiber length is 6 cm. The initial energy of laser pulses at the input of the fiber is 0.2 μJ. The dashed lines show the passbands in PCF transmission. The inset in Fig. 14a displays a cross-section image of a hollow PCF with a period of structure in the cladding of about 5 μm.

Spatial self-action of laser radiation in a medium with a Kerr nonlinearity is related to the intensity-dependent nonlinear additive to the refractive index. A spatially nonuniform distribution of radiation intensity in a laser beam propagating in a Kerr-nonlinear medium induces a profile of the refractive index, corresponding to a nonlinear lens. Kerr nonlinearity in a waveguide may result in the transformation of guided modes and lead to energy exchange between these modes.

Spatial self-action of laser radiation induced by Kerr nonlinearity may give rise to a nonlinear waveguide, where the diffraction divergence is compensated by a nonlinear lens [16]. In an unbounded domain, however, such waveguides are unstable with respect to small perturbations related to fluctuations in the parameters of laser radiation and inhomogeneities in the medium [84, 85]. Mathematically, this instability reflects the fact that the waveguide solutions of the nonlinear Schrödinger equation governing the evolution of a light beam on an unbounded domain in a nonlinear medium correspond to a zero Hamiltonian. Small fluctuations in the parameters of laser radiation or inhomogeneities in the medium under these conditions lead to beam collapse.

Reflection from the walls in a bounded area (e.g., in a capillary) stabilizes nonlinear waveguides induced by laser radiation in a medium with Kerr nonlinearity [84–86]. Waveguide solutions of the nonlinear Schrödinger equation on a bounded domain correspond to a positive Hamiltonian, which makes these solutions robust with respect to small fluctuations in the parameters of laser radiation and inhomogeneities of a medium.

Figures 15 and 16 present the results of investigation of the influence of spatial self-action on the propagation of femtosecond laser pulses through a hollow PCF. For low input laser energies, the light beam propagates through the PCF in the linear regime without spatial self-action. Insets *1* and *2* in Fig. 15 display beam patterns at the output of the hollow PCF characteristic of this regime. Output beam profiles, as can be seen from these images, represent mixtures of guided modes. As the energy of radiation coupled into the PCF increases, the output beam profile displays noticeable transformations (inset *3* in Fig. 15). The character of these transformations indicates the predominant guiding of laser radiation in circularly symmetric PCF modes.

This regime of waveguiding is observed within a limited range of input laser powers. Starting with a certain threshold initial power $P_{\rm th}$, which depends on the kind of and the pressure of the gas filling the fiber core,

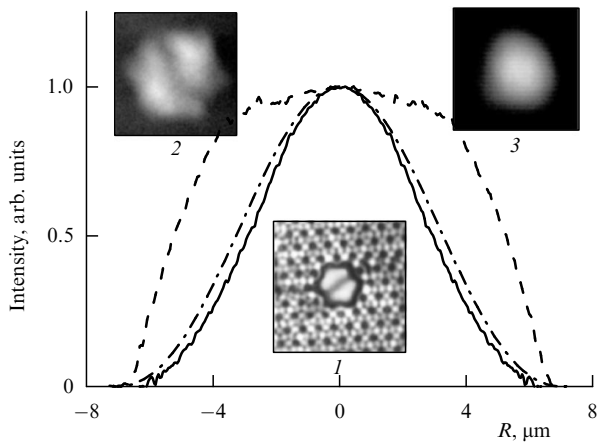

Figure 15. Radial field-intensity profiles measured at the output of a 6-cm photonic-crystal fiber filled with atmospheric-pressure air. The initial energy of laser pulses at the input of the fiber is 0.5 μJ (dashed line) and 4.0 μJ (solid line). The dash – dotted line shows the profile of the ground-state solution $Q_\beta^{(0)}$. The insets present the images of the output beam measured with (*1*) 0.1-μJ, (*2*) 0.5-μJ, and (*3*) 4-μJ femtosecond pulses at the input of the fiber.

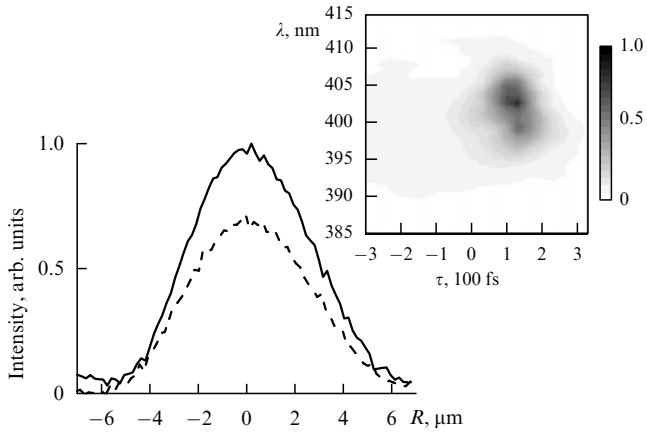

Figure 16. Radial field-intensity profiles measured at the output of a 6-cm argon-filled photonic-crystal fiber at a gas pressure of 4 atm (dashed line) and 7 atm (solid line). The initial energy of laser pulses at the input of the fiber is 2 μJ. The inset shows a cross-correlation FROG trace of the Ti: sapphire laser pulse transmitted through a 6-cm hollow PCF filled with argon at a pressure of 3 atm. The initial pulse energy is 2 μJ.

the output beam profile becomes unstable, suggesting the occurrence of an optical breakdown induced by a collapsing laser beam. The blowup threshold $P_{\rm th}$ for laser beams undergoing self-focusing in a hollow PCF was approximately two times lower than the blowup threshold for laser beams in a gas without a fiber, which agrees well with the predictions of the theory of self-focusing on bounded domains [84, 85].

Comparison of the beam profiles measured at the output of an argon-filled PCF for input pulses with low ($P < P_{\rm th}$) and subcritical [$P \approx (0.5-0.9)\,P_{\rm th}$] laser powers P (Figs 15, 16) suggests that femtosecond pulses induce a waveguide inside the hollow core of the PCF due to the Kerr nonlinearity of the gas. This effect is enhanced when the nonlinearity of the fiber core is increased at higher gas pressures (Fig. 16). Regardless of the transverse field intensity distribution at the input of the PCF, the output beam pattern in the regime of subcritical laser powers tends to a circularly symmetric profile. To assess distortions in the temporal structure of the pulse transmitted through the PCF, we applied the cross-correlation frequency-resolved optical gating (XFROG) [87] technique. An XFROG trace of the output pulse measured using a 50-fs pulse from a Ti: sapphire laser as a reference field demonstrates (inset in Fig. 16) that the pulses transmitted through the PCF have a smooth envelope with a typical width of about 60 fs.

We now interpret the results of our experiments in terms of the theory of self-focusing on bounded domain [84–86]. Define nondimensional cylindrical coordinates r and z as

$$r = \frac{R}{R_0}\,, \quad z = \frac{Z}{L_{\rm df}}\,,$$

where R is the dimensional radial coordinate, R_0 is the inner radius of the hollow fiber, Z is the dimensional longitudinal coordinate, and $L_{\rm df} = k_0 R_0^2$ is the diffraction length ($k_0 = \omega_0 n_0/c$ is the wave number, ω_0 is the radiation frequency, and n_0 is the field-unperturbed refractive index).

The radial profiles of light intensity distribution in the modes $\psi \propto \exp(\mathrm{i}\beta z)\,Q_\beta(r)$ of waveguides induced through

Kerr nonlinearity along the z-axis on a bounded domain with a circular symmetry are described [85] by the solutions $Q_\beta(r)$ to the ordinary differential equation

$$\Delta_\perp Q_\beta - \beta Q_\beta + Q_\beta^3 = 0\,, \quad \Delta_\perp = \frac{\partial^2}{\partial r^2} + \frac{1}{r}\frac{\partial}{\partial r}\,,$$

subject to boundary conditions

$$\frac{\mathrm{d}Q_\beta(0)}{\mathrm{d}r} = 0\,, \quad Q_\beta(1) = 0\,,$$

which neglect the electromagnetic field propagating outside the fiber core. This differential equation has an infinite number of solutions $Q_\beta^{(n)}$, $n = 0, 1, 2, \ldots$. The Hamiltonians for all the guided modes $Q_\beta^{(n)}$ are positive, preventing the blowup of these solutions in the presence of small fluctuations [84], thus stabilizing the nonlinear waveguides in a hollow fiber.

The ground-state solution $Q_\beta^{(0)}$ is strictly positive for $1 \geqslant r \geqslant 0$ and is a monotonically decreasing function of r, tending to a zeroth-order Bessel function in the case of low field amplitudes,

$$Q_\beta^{(0)} \propto \varepsilon J_0(2.4r)\,,$$

where ε is a small parameter, controlled by the field intensity and the nonlinearity of the gas filling the fiber. The radial profile of field intensity in such a ground-state waveguide (shown by the dash–dotted line in Fig. 15) provides a good approximation for the experimental beam profile at the output of the hollow PCF (the solid line in Fig. 15).

Although the modes $Q_\beta^{(n)}$ are stable with respect to small perturbations, these solutions are centers, rather than attractors, in a conservative system [84]. However, mode solutions corresponding to Kerr-nonlinearity-induced waveguides may become attractors in systems with dissipation [86], e.g., in hollow PCFs with losses. The circularly symmetric field distribution is then formed at the output of the PCF regardless of the initial beam profile. In the experiments described above, this effect shows up as intensity-dependent modes guided in hollow PCFs.

A similar universal behavior has been recently demonstrated by Moll et al. [88] for collapsing light beams, tending to form Townesian profiles [16] with no memory of the initial intensity profile while undergoing self-focusing on an infinite domain in bulk materials. Unlike Townesian beam profiles, which are known to be unstable in free space, the ground-state waveguide modes observed in hollow PCFs in the regime of subcritical laser powers remained stable with respect to small fluctuations, resulting in no blowup until the critical power P_{th} was reached.

The results of the experiments presented in this section demonstrate the influence of spatiotemporal self-action effects on the transmission of high-intensity ultrashort pulses through hollow-core PCFs. Hollow PCFs providing a waveguide regime of nonlinear-optical interactions for femtosecond pulses of 800-nm radiation have been designed and fabricated. Experimental studies show that a light-induced change in the refractive index of a gas filling the PCF core not only leads to the spectral broadening of laser pulses due to self-phase modulation, but also suggests ways of guiding high-intensity ultrashort laser pulses in the regime of self-channeling.

6. Coherent excitation and probing of Raman-active molecular vibrations by air-guided modes of hollow photonic-crystal fibers

Raman scattering, discovered by Raman and Krishnan [89] and independently studied by Landsberg and Mandelstam [90], is currently widely employed as one of the most convenient, efficient, and informative methods of spectroscopy and microscopy. Coherent Raman transitions are one of the most important pathways of laser–matter interactions.

Discovery of stimulated [91–93] and coherent [94] regimes of Raman scattering gave rise to new powerful spectroscopic and time-resolved laser techniques for the investigation of ultrafast energy-transfer processes in molecular and atomic systems [95–100], as well as methods of quantum control [101, 102], laser cooling of atoms [103, 104], and efficient frequency conversion of laser radiation [20, 99]. High-order stimulated Raman scattering is currently considered as one of the promising means of ultrashort pulse synthesis, offering interesting strategies for the generation of subfemtosecond and attosecond field waveforms [25, 105–110]. The potential of nonlinear Raman techniques (see inset *1* in Fig. 17) is now enhanced by coherent control approaches, extended recently to coherent anti-Stokes Raman scattering [111, 112].

Waveguide coherent Raman scattering [30, 113, 114] offers new ways to radically improve the sensitivity of spectroscopic and time-resolved techniques, as well as to increase the efficiency of frequency conversion and ultrashort-pulse generation. Hollow fibers have been shown to substantially enhance coherent Raman scattering in the gas phase. Multimode regimes of waveguiding typical of such fibers (see Section 1 of this review), however, lead to unwanted interference phenomena, limiting the sensitivity and selectivity of spectroscopic and time-resolved methods, as well as coherence- and quantum-control schemes. In particular, the difference in phase and group velocities of waveguide modes simultaneously excited in a standard

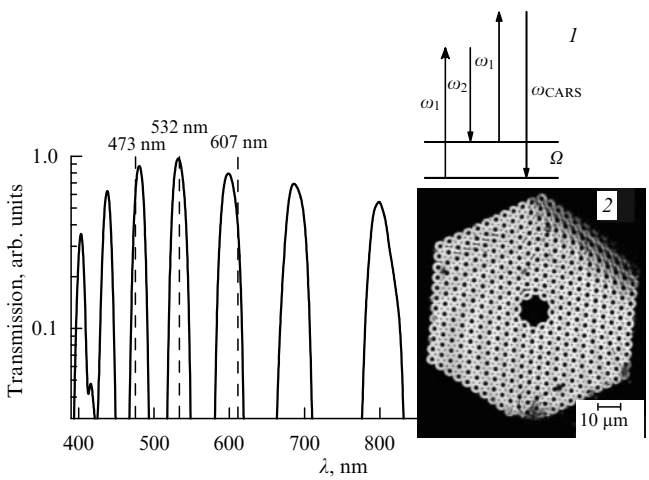

Figure 17. Transmission spectrum of the hollow PCF designed to simultaneously support air-guided modes of the pump, probe, and CARS signal fields (the wavelengths of these fields are shown by the vertical dashed lines) in the hollow core of the fiber. The insets show (*1*) a diagram of the CARS process and (*2*) an image of the PCF cross section.

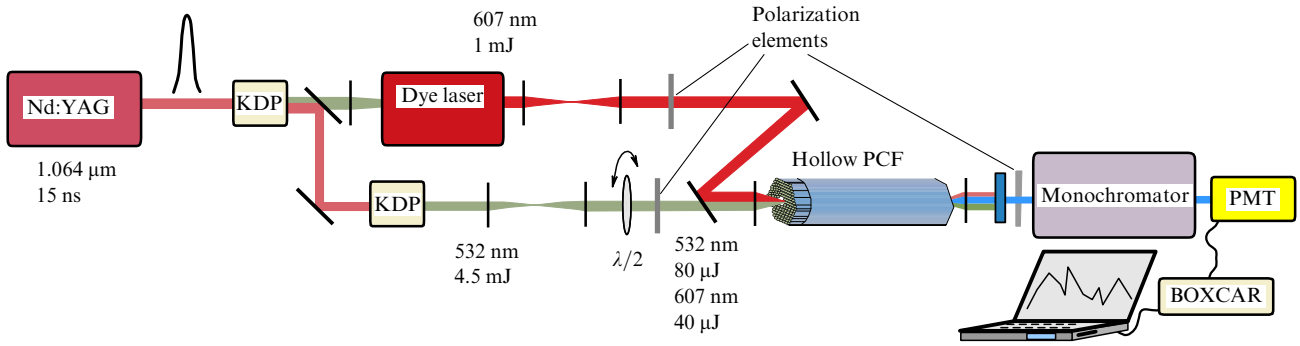

Figure 18. Diagram of the laser setup for coherent excitation and probing of Raman-active vibrations in the gas phase by isolated air-guided modes of a hollow PCF.

hollow fiber gives rise to uncertainties in time-resolved measurements and complicates the calibration of the nonlinear signal as a function of the gas pressure [32, 33]. Thus, although conventional, solid-cladding hollow fibers can provide very high levels of nonlinear signals, quantitative analysis of gas media and time-resolved measurements based on nonlinear-optical processes in such fibers often encounter serious difficulties.

In this section, we will discuss the possibility of using isolated air-guided modes of hollow-core PCFs to coherently excite and probe Raman-active vibrations in the gas phase. The results of experiments [115], discussed below in this section, indicate a radical enhancement of CARS in hollow PCFs. The intensity of the CARS signal generated in a 3-cm hollow PCF by nanosecond pump pulses whose frequency difference is tuned to a Raman resonance with vibrational transitions in molecular nitrogen is shown to be 5 to 7 times higher than the intensity of the CARS signal in the regime of tight focusing.

Hollow PCFs employed for the CARS spectroscopy of molecular nitrogen [115] had a photonic-crystal cladding with a period of 5 μm and a hollow core with a diameter of 14 μm. A typical cross-section image of such a PCF is shown in inset *2* in Fig. 17. The manifold of passbands in the transmission spectra of PCFs was adjusted, through PCF structure engineering, in such a way as to simultaneously support air-guided modes of the second harmonic of an Nd : YAG laser (with a wavelength of 532 nm), tunable dye-laser radiation (600 – 610 nm), and the CARS signal (473 nm). The PCF length in these experiments was equal to 3 cm.

Spectroscopic measurements were performed with the use of a standard two-color CARS technique, involving detection of the anti-Stokes signal at the frequency $\omega_{\mathrm{CARS}} = 2\omega_1 - \omega_2$, where ω_1 and ω_2 are the frequencies of the pump fields. A Q-switched Nd : YAG master oscillator employed in these experiments generated 15-ns pulses of 1.064 μm radiation (Fig. 18), which were then amplified and converted into the second harmonic with a KDP crystal.

The second harmonic served as one of the pump fields in the CARS process (frequency ω_1). Fundamental radiation that remained frequency-unconverted at the output of the nonlinear crystal was separated from the second harmonic with a dichroic mirror and employed to generate the second harmonic in the second KDP crystal. This second-harmonic beam was then used to pump a sulforhodamine-101 dye laser. Dye-laser radiation served as the second pump field in the CARS process (frequency ω_2). Pump fields with frequencies ω_1 and ω_2 were brought to spatial coincidence with a dichroic mirror and were coupled into the hollow PCF with a spherical lens. The energies of the second-harmonic and dye-laser pulses were varied within the ranges of 10 – 200 and 10 – 80 μJ, respectively.

The frequency ω_2 of dye-laser radiation was chosen in such a way as to satisfy the condition of Raman resonance, $\omega_1 - \omega_2 = \Omega$, with a Raman-active transition of molecular nitrogen with $\Omega = 2331\ \mathrm{cm}^{-1}$ (inset *1* in Fig. 17). This condition was met with the wavelength of dye-laser radiation equal to 607 nm. The wavelength of the CARS signal related to molecular nitrogen in the atmospheric-pressure air filling the hollow PCF was then equal to 473 nm. This signal was collimated with a spherical lens and separated from the pump beams with a set of optical filters. The spectrum of the CARS signal was measured with the use of a monochromator and an optical multichannel analyzer.

The pump fields with frequencies ω_1 and ω_2 coherently excite Raman-active vibrations of nitrogen molecules in the atmospheric-pressure air filling the hollow core of the PCF. These coherently excited vibrations then scatter off the probe field with the frequency ω_1, giving rise to the anti-Stokes signal. The spectrum of this coherently scattered signal is shown in Fig. 19. The energy of the CARS signal produced in a hollow-core PCF was compared with the energy of the CARS signal generated by tightly focused second-harmonic and dye-laser beams with the same energies. This comparison allowed the waveguide CARS enhancement factor to be

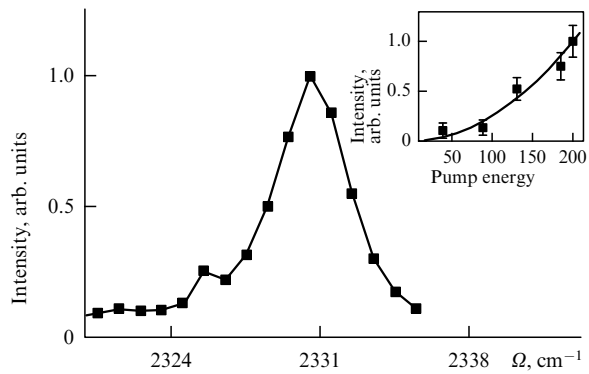

Figure 19. CARS spectrum of Q-branch Raman-active vibrations of nitrogen molecules in atmospheric-pressure air filling the hollow core of the PCF. The inset shows the CARS intensity as a function of the energy of the second-harmonic field.

estimated as 5–7 for the above-specified experimental conditions.

The mismatch of the propagation constants of the waveguide modes involved in the CARS process is the main physical factor limiting the efficiency of nonlinear-optical interaction in the experiments described above. In view of the $\lambda^2 l^2/a^4$ scaling law [116] of waveguide CARS enhancement in hollow PCFs (λ is the radiation wavelength, l is the nonlinear interaction length, and a is the fiber core radius), we can scale up the results of our measurements to predict waveguide CARS enhancement by a factor of about 500 in hollow-core PCFs with mode dispersion profiles engineered to increase the CARS coherence length up to approximately 30 cm. The inset in Fig. 19 presents the CARS signal intensity measured as a function of the second-harmonic energy. A quadratic function provides an ideal fit for this dependence, indicating that the contribution of competing nonlinear-optical processes is negligibly small.

Experimental results presented in this work demonstrate that hollow-core PCFs can radically enhance coherent anti-Stokes Raman scattering in the gas phase. Photonic-crystal fibers thus suggest ways of substantially improving the sensitivity of nonlinear spectroscopy of gas media, allowing the energy requirements to laser pump beams to be considerably loosened. The experiments presented above also show that a hollow PCF can combine a waveguide component, increasing the length of nonlinear-optical interactions, with a passband filter, selecting the anti-Stokes signal produced through CARS against background emission. This filtering option offered by hollow PCFs can be employed for a further improvement of the sensitivity of nonlinear spectroscopic methods.

7. Conclusion

The invention of lasers provided an opportunity to generate directed coherent optical radiation — a powerful means for fundamental research and advanced technologies. Fiber-optic components make it possible to overcome the natural diffraction divergence of laser radiation, allowing transportation of laser light over large distances and creation of highly efficient and practical systems for the transmission and processing of optical signals and information. The progress toward higher intensities and shorter pulse durations is one of the main tendencies in laser optics, offering new exciting possibilities for the investigation of the fundamental aspects of light–matter interactions and the development of new revolutionary optical technologies.

Transmission of high-intensity laser pulses over large distances and control of such pulses require radically new solutions in the physics of guided waves. Hollow photonic-crystal fibers, developed in the late 1990s, can for the first time produce robust isolated air-guided modes of subgigawatt ultrashort laser pulses. These fibers allow highly efficient nonlinear-optical transformations of isolated air-guided modes of high-intensity laser fields, suggesting ways of using these states of high-intensity fields for coherent excitation and probing of molecular vibrations in the waveguide regime.

The results of experimental and theoretical studies presented in this review show that hollow-core PCFs with a special dispersion profile allow phase-matched nonlinear-optical interactions of isolated air-guided modes of high-intensity femtosecond laser pulses confined in the hollow fiber core. This phase matching of isolated air-guided modes of high-intensity femtosecond laser pulses involved in nonlinear-optical interactions in a hollow PCF provides a high efficiency of frequency conversion for ultrashort laser pulses with an intensity on the order of 10^{14} W cm^{-2} and stabilizes the spatial intensity profile of the output FWM signal.

Results of experimental studies demonstrate the influence of spatiotemporal self-action effects on the transmission of high-intensity ultrashort pulses through hollow-core PCFs. The light-induced change in the refractive index of a gas filling the PCF core not only leads to the spectral broadening of laser pulses due to self-phase modulation, but also suggests ways of guiding high-intensity ultrashort laser pulses in the regime of self-channeling. Coherent anti-Stokes Raman scattering in hollow-core PCFs has been experimentally demonstrated, suggesting the unique possibility of coherent excitation and probing of Raman-active molecular vibrations in the gas phase by isolated guided modes of electromagnetic radiation. The waveguide regime of nonlinear-optical interactions in isolated guided modes of hollow PCFs radically enhances coherent anti-Stokes Raman scattering relative to the regime of tight focusing, offering ways of substantially improving the sensitivity of coherent Raman scattering spectroscopy.

I am pleased to gratefully acknowledge fruitful collaboration and illuminating discussions with S O Konorov, E E Serebryannikov, A B Fedotov, D A Sidorov-Biryukov, D A Akimov, and V P Mitrokhin (Physics Department, M V Lomonosov Moscow State University); A A Ivanov and M V Alfimov (Center of Photochemistry, Russian Academy of Sciences); D von der Linde and A P Tarasevitch (University of Essen–Duisburg); R Miles (Princeton University); P Russell (University of Bath); M Scalora (Redstone Arsenal, Huntsville); V I Beloglazov, N B Skibina, and A V Shcherbakov (Institute of Technology and Equipment for Glass Structures, Saratov); D Chorvat, D Chorvat Jr., and I Bugar (International Laser Center, Bratislava); E Wintner (Technical University, Vienna); and L A Mel'nikov (N G Chernyshevsky Saratov State University).

This study was supported in part by the President of the Russian Federation Grant MD-42.2003.02, the Russian Foundation for Basic Research (projects Nos. 03-02-16929, 04-02-81036-Bel2004, and 03-02-20002-BNTS), and INTAS (projects Nos. 03-51-5037 and 03-51-5288). The research described in this publication was made possible in part by award No. RP2-2558 of the U.S. Civilian Research & Development foundation for the Independent States of the Former Soviet Union (CRDF). This material is also based upon work supported by the European Research Office of the US Army under Contract No. 62558-04-P-6043.

References

1. *Euclidis Optica & Catoptrica* (è Greco versa per I Penam) (Parisüs: Apud Andream Wechelum, 1557)
2. Einstein A *Mitteil. Phys. Gesellschaft Zürich* **16** 47 (1916)
3. Ladenburg R *Z. Phys.* **48** 15 (1928)
4. Basov N G, Prokhorov A M *Zh. Eksp. Teor. Fiz.* **27** 431 (1954)
5. Schawlow A L, Townes C H *Phys. Rev.* **112** 1940 (1958)
6. Maiman T H *Nature* **187** 493 (1960)
7. Fresnel A J *Oeuvres complètes d'Augustin Fresnel* Vol. 1 (Paris: Imprimerie Impériale, 1866) p. 17
8. Hondros D, Debye P *Ann. Phys.* (Leipzig) **32** 465 (1910)
9. Snyder A W, Love J D *Optical Waveguide Theory* (London: Chapman and Hall, 1983)
10. Adams M J *An Introduction to Optical Waveguides* (Chichester: Wiley, 1981)
11. Dianov E M, in *Spravochnik po Lazeram* (Laser Handbook) Vol. 3 (Ed A M Prokhorov) (Moscow: Sov. Radio, 1978) p. 108; see also

Handbook of Laser with Selected Data on Optical Technology (Ed. R J Pressley) (Cleveland: Chemical Rubber Co., 1971)
12. Tajima T, Mourou G *Phys. Rev. ST Accel. Beams* **5** 031301 (2002)
13. Askar'yan G A *Zh. Eksp. Teor. Fiz.* **42** 1567 (1962) [*Sov. Phys. JETP* **15** 1088 (1962)]
14. Hercher M *J. Opt. Soc. Am.* **54** 563 (1964)
15. Pilipetskiĭ N F, Rustamov A R *Pis'ma Zh. Eksp. Teor. Fiz.* **2** 88 (1965) [*JETP Lett.* **2** 55 (1965)]
16. Chiao R Y, Garmire E, Townes C H *Phys. Rev. Lett.* **13** 479 (1964)
17. Lugovoĭ V N, Prokhorov A M *Pis'ma Zh. Eksp. Teor. Fiz.* **7** 153 (1968) [*JETP Lett.* **7** 117 (1968)]
18. Loy M M T, Shen Y R *Phys. Rev. Lett.* **22** 994 (1969)
19. Akhmanov S A, Sukhorukov A P, Khokhlov R V *Usp. Fiz. Nauk* **93** 19 (1967) [*Sov. Phys. Usp.* **10** 609 (1968)]
20. Shen Y R *The Principles of Nonlinear Optics* (New York: J. Wiley, 1984) [Translated into Russian (Moscow: Nauka, 1989)]
21. Marcatili E A J, Schmeltzer R A *Bell Syst. Tech. J.* **43** 1783 (1964)
22. Zheltikov A M *Usp. Fiz. Nauk* **172** 743 (2002) [*Phys. Usp.* **45** 687 (2002)]
23. Nisoli M, De Silvestri S, Svelto O *Appl. Phys. Lett.* **68** 2793 (1996)
24. Nisoli M et al. *Opt. Lett.* **22** 522 (1997)
25. Zhavoronkov N, Korn G *Phys. Rev. Lett.* **88** 203901 (2002)
26. Rundquist A et al. *Science* **280** 1412 (1998)
27. Constant E et al. *Phys. Rev. Lett.* **82** 1668 (1999)
28. Durfee III C G et al. *Phys. Rev. Lett.* **83** 2187 (1999)
29. Paul A et al. *Nature* **421** 51 (2003)
30. Miles R B, Laufer G, Bjorklund G C *Appl. Phys. Lett.* **30** 417 (1977)
31. Fedotov A B et al. *Appl. Phys. B* **72** 575 (2001)
32. Naumov A N et al. *Zh. Eksp. Teor. Fiz.* **120** 280 (2001) [*JETP* **93** 247 (2001)]
33. Naumov A N et al. *Pis'ma Zh. Eksp. Teor. Fiz.* **73** 300 (2001) [*JETP Lett.* **73** 263 (2001)]
34. Konorov S O et al. *J. Raman Spectrosc.* **33** 955 (2002)
35. Nibbering E T J et al. *Opt. Lett.* **21** 62 (1996)
36. Brodeur A et al. *Opt. Lett.* **22** 304 (1997)
37. La Fontaine B et al. *Phys. Plasmas* **6** 1615 (1999)
38. Kasparian J et al. *Opt. Lett.* **25** 1397 (2000)
39. Rairoux P et al. *Appl. Phys. B* **71** 573 (2000)
40. Méjean G et al. *Appl. Phys. B* **77** 357 (2003)
41. Cregan R F et al. *Science* **285** 1537 (1999)
42. Russell P *Science* **299** 358 (2003)
43. Knight J C *Nature* **424** 847 (2003)
44. Smith C M et al. *Nature* **424** 657 (2003)
45. Zheltikov A M *Optika Mikrostrukturirovannykh Volokon* (Optics of Microstructure Fibers) (Moscow: Nauka, 2004)
46. Konorov S O et al. *Pis'ma Zh. Eksp. Teor. Fiz.* **76** 401 (2002) [*JETP Lett.* **76** 341 (2002)]
47. Benabid F et al. *Science* **298** 399 (2002)
48. Benabid F et al., in *Conf. on Laser Electro-Optics/Intern. Quantum Electronics Conf. & Photonic Applications, Systems and Technologies, CLEO/IQEC & PhAST 2004, May 16 – 21, 2004, San Francisco, Calif., USA*, Conf. Program, CThEE5, p. 156
49. Konorov S O, Fedotov A B, Zheltikov A M *Opt. Lett.* **28** 1448 (2003)
50. Konorov S O et al. *Appl. Phys. B* **78** 547 (2004)
51. Ouzounov D G et al. *Science* **301** 1702 (2003)
52. Luan F et al. *Opt. Express* **12** 835 (2004)
53. Benabid F, Knight J C, Russell P St J *Opt. Express* **10** 1195 (2002)
54. Konorov S O et al. *J. Phys. D: Appl. Phys.* **36** 1375 (2003)
55. Shephard J D et al. *Opt. Express* **12** 717 (2004)
56. Konorov S O et al. *Appl. Opt.* **43** 2251 (2004)
57. Bloch F *Z. Phys.* **52** 555 (1928)
58. Bragg W H, Bragg W L *X Rays and Crystal Structure* 4th ed. (London: G. Bell, 1924); Bragg W L "The diffraction of X-rays by crystals", in *Nobel Lectures. Physics, 1901 – 1921* (Amsterdam: Elsevier, 1967); http://nobelprize.org/physics/laureates/1915/wl-bragg-lecture.pdf
59. Yablonovitch E *Phys. Rev. Lett.* **58** 2059 (1987)
60. John S *Phys. Rev. Lett.* **58** 2486 (1987)
61. Sakoda K *Optical Properties of Photonic Crystals* (Berlin: Springer, 2001)
62. Bowden C M, Zheltikov A M (Eds) "Nonlinear optics of photonic crystals: feature issue" *J. Opt. Soc. Am. B* **19** (9) (2002)
63. Yeh P, Yariv A *Opt. Commun.* **19** 427 (1976)
64. Yariv A, Yeh P *Optical Waves in Crystals: Propagation and Control of Laser Radiation* (New York: Wiley, 1984) [Translated into Russian (Moscow: Mir, 1987)]
65. Serebryannikov E E, Zheltikov A M *Laser Phys.* **14** (12) (2004) (in press)
66. Mogilevtsev D, Birks T A, Russell P St J *Opt. Lett.* **23** 1662 (1998)
67. Monro T M et al. *J. Lightwave Technol.* **17** 1093 (1999)
68. Monro T M et al. *J. Lightwave Technol.* **18** 50 (2000)
69. Konorov S O et al. *Zh. Eksp. Teor. Fiz.* **123** 975 (2003) [*JETP* **96** 857 (2003)]
70. Broeng J et al. *Opt. Lett.* **25** 96 (2000)
71. Konorov S O et al. *Laser Phys. Lett.* **1** 548 (2004)
72. Konorov S O et al. *Laser Phys.* **13** 1046 (2003)
73. Konorov S O et al. *Laser Phys.* **14** 780 (2004)
74. Spielmann Ch et al. *Science* **278** 661 (1997)
75. Chang Z et al. *Phys. Rev. Lett.* **79** 2967 (1997)
76. Paul P M et al. *Science* **292** 1689 (2001)
77. Drescher M et al. *Science* **291** 1923 (2001)
78. Hentschel M et al. *Nature* **414** 509 (2001)
79. Zheltikov A M *Usp. Fiz. Nauk* **174** 73 (2004) [*Phys. Usp.* **47** 69 (2004)]
80. Konorov S O et al. *Pis'ma Zh. Eksp. Teor. Fiz.* **79** 499 (2004) [*JETP Lett.* **79** 395 (2004)]
81. Serebryannikov E E, von der Linde D, Zheltikov A M *Phys. Rev. E* **70** 061412 (2004)
82. Konorov S O et al. *Phys. Rev. A* **70** 023807 (2004)
83. Konorov S O et al. *Opt. Lett.* **29** 1521 (2004)
84. Fibich G, Merle F *Physica D* **155** 132 (2001)
85. Fibich G, Gaeta A L *Opt. Lett.* **25** 335 (2000)
86. Fibich G *SIAM J. Appl. Math.* **61** 1680 (2001)
87. Dudley J M et al. *Opt. Express* **10** 1215 (2002)
88. Moll K D, Gaeta A L, Fibich G *Phys. Rev. Lett.* **90** 203902 (2003)
89. Raman C V, Krishnan K S *Nature* **121** 501 (1928)
90. Landsberg G S, Mandelstam L I *Naturwissenschaften* **16** 557 (1928)
91. Woodbury E J, Ng W K *Proc. IRE* **50** 2347 (1962)
92. Hellwarth R W *Phys. Rev.* **130** 1850 (1963)
93. Garmire E, Pandarese F, Townes C H *Phys. Rev. Lett.* **11** 160 (1963)
94. Maker P D, Terhune R W *Phys. Rev.* **137** A801 (1965)
95. Akhmanov S A, Koroteev N I *Metody Nelineĭnoĭ Optiki v Spektroskopii Rasseyaniya Sveta: Aktivnaya Spektroskopiya Rasseyaniya Sveta* (Methods of Nonlinear Optics in Light Scattering Spectroscopy: Active Spectroscopy of Light Scattering) (Moscow: Nauka, 1981)
96. Eesley G L *Coherent Raman Spectroscopy* (Oxford: Pergamon Press, 1981)
97. Druet S A J, Taran J-P E *Prog. Quantum Electron.* **7** 1 (1981)
98. Eckbreth A C *Laser Diagnostics for Combustion Temperature and Species* (Energy and Engineering Science Ser., Vol. 7) (Cambridge, Mass.: Abacus Press, 1988)
99. Zheltikov A M, Koroteev N I *Usp. Fiz. Nauk* **169** 385 (1999) [*Phys. Usp.* **42** 321 (1999)]
100. Zheltikov A M, in *Handbook of Vibrational Spectroscopy* Vol. 1 (Eds J M Chalmers, P R Griffiths) (New York: J. Wiley, 2002) p. 572
101. Kiefer W (Ed.) "Femtosecond coherent Raman spectroscopy: special issue" *J. Raman Spectrosc.* **31** (1/2) (2000)
102. Zeidler D et al. *J. Chem. Phys.* **116** 5231 (2002)
103. Heinzen D J, Wineland D J *Phys. Rev. A* **42** 2977 (1990)
104. Monroe C et al. *Phys. Rev. Lett.* **75** 4011 (1995)
105. Harris S E, Sokolov A V *Phys. Rev. Lett.* **81** 2894 (1998)
106. Sokolov A V, Yavuz D D, Harris S E *Opt. Lett.* **24** 557 (1999)
107. Sokolov A V et al. *Phys. Rev. Lett.* **85** 562 (2000)
108. Nazarkin A, Korn G *Phys. Rev. A* **58** R61 (1998)
109. Korn G, Dühr O, Nazarkin A *Phys. Rev. Lett.* **81** 1215 (1998)
110. Nazarkin A et al. *Phys. Rev. Lett.* **83** 2560 (1999)
111. Oron D et al. *Phys. Rev. A* **65** 043408 (2002)
112. Dudovich N, Oron D, Silberberg Y *Nature* **418** 512 (2002)
113. Stegeman G I et al. *Opt. Lett.* **8** 295 (1983)
114. de Boeij W P et al. *Appl. Spectrosc.* **47** 723 (1993)
115. Fedotov A B et al. *Phys. Rev. A* **70** 045802 (2004)
116. Zheltikov A M *Zh. Eksp. Teor. Fiz.* **124** 558 (2003) [*JETP* **97** 505 (2003)]